Preface and acknowledgements

The experimental work and writing presented in this master's thesis have been conducted in the Chemosensory laboratory at the Department of Psychology (Norwegian University of Technology and Science). Through this work, I have had an opportunity of studying an area of science that fascinates me endlessly: the nervous system. I am very grateful for this opportunity. I would like to thank my fellow lab members for a truly interesting, rewarding, and deeply satisfying experience. Particularly, my main supervisor Xi Chu and Ph.D. student Jonas Kymre Hansen have both been enormously helpful in teaching the how to perform experiments, interpreting the results and provided insightful conversations. Their aid have greatly improved this master's thesis, and for that you have my sincerest thanks.

My co-supervisor and leader of the Chemosensory lab, Professor Bente G. Berg, have provided plenty of thoughtful conversations and feedback on my work, which have helped me in understanding how the olfactory system work, from the periphery to higher brain areas. For this, I am very grateful. I would also like to thank Elena Ian, Pramod KC, Hanna Mustaparta, and Ina Saltvik for your many thoughtful inputs to my work and enjoyable conversations regarding olfaction but also non-science related topics. As for my fellow master student, Ina Saltvik, I thank you for your help in the methodological procedures, especially in testing and developing the microelectrode used for intracellular recording. Lastly, I would direct a very special thanks to Maria, which have put up with my obsession with neural science for quite some time, especially this last year. Your unconditional support of my scientific dreams and ambitions have been very much appreciated and I am forever grateful.

Christoffer Nerland Berge

Abstract

In the insect brain, different types of neurons provide input and output to the primary olfactory center, the antennal lobe. The principal output neurons, projection neurons, convey odor information from the antennal lobe to higher brain areas by projecting in one of six parallel tracts (m-ALT, ml-ALT, l-ALT, t-ALT, d-ALT, and dm-ALT). In turn, centrifugal neurons innervating higher brain areas provide input to, and modulate, the processing in the antennal lobe. However, the functional role of the parallel tracts and centrifugal neurons in olfactory processing, is yet poorly understood. Here, we have investigated these two types of neurons in the noctuid moth *Helicoverpa Armigera*, by using *in vivo* intracellular recording and iontophoretic staining of individual neurons, in combination with confocal microscopy. The results demonstrate that morphologically diverse projection neurons shows different physiological responses to different odors. This suggests that individual tracts are associated with distinct functional roles. Neurons in the m-ALT are more narrowly tuned to odors and appeared to encode odor identity, whereas ml-ALT and l-ALT are more broadly tuned as serve other functions. In addition, the comparison of output area of pheromone-sensitive projection neurons confined to the m-ALT in the lateral protocerebrum showed non-overlapping terminal regions with the non-pheromone m-ALT projection neurons. Projection neurons exhibited several different physiological response patterns in response to odors. This suggests that individual projection neurons may encode various features of the olfactory stimuli through different response patterns. The labelling and identification of a new centrifugal neuron, the bilateral, paired centrifugal neuron, indicates that this neuron respond directly to the olfactory pathways and may serve as a feedback neuron. Contrary, the CSD neuron exhibited no response to any of the tested odors, which suggests that this neuron influence AL processing based on internal states of the animal or non-olfactory input, rather than a direct connection with olfactory pathways.

Abbreviations

αL	Alpha-lobe
ACC	Anterior cell cluster
AL	Antennal lobe
ALT	Antennal lobe tract
AVLP	Anterior ventro-lateral protocerebrum
βL	Beta-lobe
BPC	Bilateral, paired centrifugal neuron
Ca	Calyces
CB	Central body
CN	Centrifugal neuron
CSD neuron	Contralaterally projecting, serotonin-immunoreactive deutocerebral neuron
d-ALT	Dorsal antennal-lobe tract
dm-ALT	Dorso-medial antennal-lobe tract
γL	Gamma-lobe
GABA	γ-aminobutyric acid
INP	Inferior neuropil
l-ALT	Lateral antennal-lobe tract
LAL	Lateral accessory lobe
LCC	Lateral cell cluster
LLE	Long-lasting excitation
LH	Lateral horn
LN	Local interneuron
m-ALT	Medial antennal-lobe tract
MB	Mushroom bodies
MCC	Medial cell cluster
MGC	Macroglomerular complex
ml-ALT	Medio-lateral antennal lobe tract
OG	Ordinary glomeruli
OSN	Olfactory sensory neuron
PLP	Posterior lateral protocerebrum
PN	Projection neuron

PSTH	Peri-stimulus time histogram
PVLP	Posterior ventro-lateral protocerebrum
SIP	Superior intermediate protocerebrum
SLP	Superior lateral protocerebrum
SMP	Superior medial protocerebrum
SNP	Superior neuropil
VMPN	Ventro-medial neuropil
VUM neuron	Ventral unpaired median neuron
t-ALT	Transverse antennal-lobe tract

Table of Contents

1. Introduction

1.1 Olfaction guides a wide range of behaviors

An organism's ability to successfully navigate in its environment, e.g., find a suitable mate, avoid predators, and seek out sources of food, depends on how well it is able to detect and respond to relevant signals from the external world. In both vertebrates and invertebrates, the identification and discrimination of odors through the sense of smell (olfaction) guides a wide range of behaviors, including mate selection, sexual behavior, foraging, and terrestrial formation and maintenance (reviewed by Doty, 1986; Hartlieb & Anderson, 1999). For instance, the presence of fox-urine components elicits avoidant behavior in rats (Wernecke et al., 2015). In many insect species, sex pheromones released by the female evokes attractive, searching behaviors in conspecific males (reviewed by Shorey, 1973).

1.1.1 Olfaction in vertebrates and invertebrates

The structural and functional organization of the olfactory system in vertebrates and invertebrates share a similar set of principles, as shown in Figure 1, which is observed across many levels of the neural circuits, from the peripheral detection of odors to processing in higher brain areas (reviewed by Ache & Young, 2005; Hildebrand & Shepherd, 1997). In mammals, olfactory sensory neurons (OSNs) in the olfactory epithelium project to the primary processing center, the olfactory bulb. Mitral and tufted cells then convey odor signals to multiple higher brain areas including the cortical amygdala and piriform cortex, (Choi et al., 2011; Root, Denny, Hen, & Axel, 2014). In the insect brain, OSNs located in the antennae transfer odor signals from sensillum to the antennal lobe (AL; analogous to the olfactory bulb in mammals) (reviewed by Wilson & Mainen, 2006). In turn, second-order projection neurons (PNs) corresponding to the mitral and tufted cells, send odor signals to the calyces of the mushroom bodies and lateral horn (LH). The calyces correspond to the cortical amygdala in mammals, and serves as a memory center associated with learned odor-evoked behaviors. The LH, as the mammalian piriform cortex, is associated with innate odor-evoked behaviors. Furthermore, olfactory processing in both the olfactory bulb and the AL is modulated by centrifugal neurons (CNs), which receive input from secondary olfactory processing centers and other brain regions.

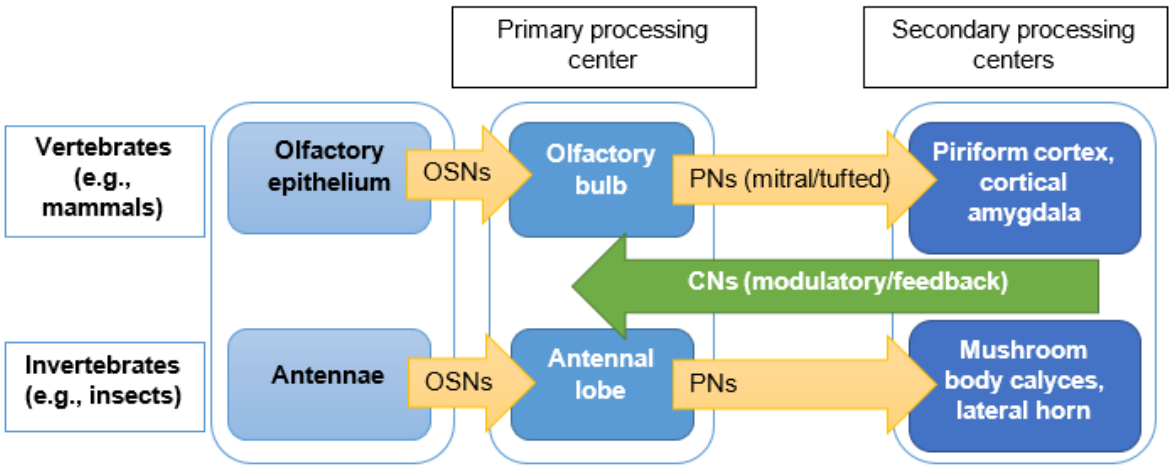

Figure 1. Schematic model of the olfactory systems of vertebrates and invertebrates. In both organisms, odors are detected by olfactory sensory neurons (OSNs) and transferred to the primary olfactory center. Then, projection neurons (PNs) convey odor information to higher brain areas associated with learned or innate odor-evoked behaviors. Centrifugal neurons (CNs) provide top-down modulation/feedback from higher brain areas to the primary processing center.

1.1.2 Insects as model organisms in olfactory research

As the olfactory system in phylogenetically diverse organisms share many similarities, a wide range of animal models have been used to study the neural principles underlying olfaction. Insects are particularly suitable model organisms in olfactory research due to their relatively simple and accessible nervous systems, and robust behavioral responses to biologically relevant odors (reviewed by Martin et al., 2011). Holometabolous insects belonging to the order of lepidoptera (moth) are frequently used in studies of the olfactory system due to their excellent sense of smell and their stereotypical behavioral responses to pheromones (reviewed by Hansson, 1995). Pheromones are chemical compounds that serve as communication signals within a species (intra-specific communication) (Wyatt, 2003). In moths, a single pheromone molecule is sufficient to generate an action potential in sensory neurons in male moths, and they can detect and locate a female from a distance of 1km by following the pheromone plume (reviewed by Kaissling, 2014). As males detect the pheromone plume, they exhibit a characteristic, zigzag upwind flying towards the pheromone source. The blend of sex pheromones released by female moths consists of one primary component and one or several minor components. The identity and ratio of the chemical components in a pheromone blend are different depending on the species studied. Taxonomically, closely related species may use the same components but at different concentration ratios. In closely related, heterospecific males, pheromone constituents of one

species may act as behavioral antagonists that suppress upwind flight in other species. Thus, sex pheromones released by a female often elicit different behaviors in conspecific and heterospecific males. A family of closely related moths knowns as heliothine moths have proved to be useful model organisms to study olfactory processing of inter- and intraspecific chemical signaling, due to their use of similar pheromone components but at different ratios (reviewed by Berg, Zhao, & Wang, 2014).

1.2 Olfactory processing in insects

The olfactory system of moths have been extensively studied in different levels. Extensive knowledge has been reported in peripheral detection and transduction of odorants (reviewed by Stengl, 2010), to central processing in the AL (reviewed by Anton & Homberg, 1999; Hansson & Christensen, 1999), and higher brain areas (e.g., Kanzaki, Arbas, & Hildebrand, 1991; Lei, Anton, & Hansson, 2001; Lei, Chiu, & Hildebrand, 2013).

1.2.1 Detection of odors and sensory transduction by olfactory sensory neurons

Airborne, volatile odorants are detected by OSNs which are housed in specialized hair-like structures on the antennae known as sensilla (Figure 2A) (reviewed by Keil, 1999; Stengl, Ziegelberger, Beoekhoff, & Krieger, 1999). Odorants first encounter the sensillum lymph, an aqueous solution containing odor- and pheromone-binding proteins. These specialized proteins bind and transport odorants to olfactory receptors located in OSN dendrites. Each OSN generally expresses only one type of olfactory receptor (Vosshall, 2000; Vosshall, Wong, & Axel, 2000). As an odorant binds to an olfactory receptor, second messenger pathways are activated, resulting in a transduction of the chemical signal into graded electrical potentials in the OSN dendrite. If sufficiently activated, the OSN generates action potentials, which travels through the antennal nerve into the AL. In mammals, the majority of OSNs are narrowly tuned to recognize a small group of odorants that share one or several structural characteristics, while a minority of OSNs are more broadly tuned and recognizes multiple odorants (Nara, Saraiva, Ye, & Buck, 2011). In heliothine moths, OSNs have been functionally characterized by responding to one key plant odorant, and weakly to a few others of similar molecular structure (Røstelien, Borg-Karlson, Fäldt, Jacobsson, & Mustaparta, 2000; Røstelien, Stranden, Borg-Karlson, & Mustaparta, 2005; Stranden et al., 2003a; Stranden et al., 2003b). Importantly, different functional subsets of OSNs exhibit no overlap of the response spectra. The specificity that applies to OSNs detecting plant volatiles

also applies to those detecting sex pheromones (Berg et al., 2014). In the male moth, *Helicoverpa armigera*, distinct subsets of OSNs are tuned primarily to the primary pheromone component (*cis*-11-hexadecenal; Z11-16:AL), the secondary component (*cis*-9-hexadecenal; Z9-16:AL), and the interspecific signal (*cis*-9-tetradecenal; Z9-14:AL), respectively (Berg et al., 2014). In other insect species, OSNs which are more broadly tuned to plant odorants have also been shown, in addition to the more narrowly tuned OSNs (reviewed by Hansson & Stensmyr, 2011)

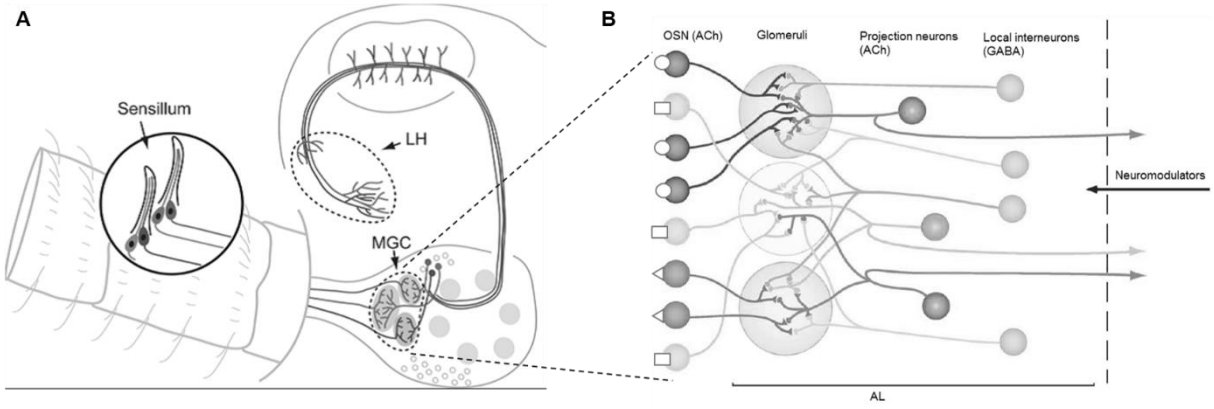

Figure 2. Overview of the olfactory pathway from the periphery to the antennal lobe in insects. **(A)** OSNs are located in hair-like structures on the antennae known as sensillum. The OSNs project via the antennal nerve to the antennal lobe, where they form dendrites in glomeruli. **(B)** All OSNs expressing the same olfactory receptor (indicated by different geometrical shapes) project to the same glomeruli. In the glomeruli the form synaptic connections with modulatory local interneurons (LNs) and projection neurons (PNs), which acts as the principal output neurons. LH, lateral horn; MGC, macroglomerular complex; AL, antennal lobe, ACh, acetylcholine; GABA, γ-aminobutyric acid; LH, lateral horn; MGC, macroglomerular complex; OSN, olfactory sensory neuron. Modified from Berg et al. (2014) and Kay et al. (2011)

1.2.2 Neuronal elements of the antennal lobe

The antennal lobe (AL), the primary olfactory processing center in the insect brain, consists of various neurons associated with specific functions. Here. the axons of OSNs converge onto spherical neuropil structures called glomeruli (see Figure 2) (Anton & Homberg, 1999). All OSNs expressing a particular olfactory receptor type projects to 1-2 glomeruli. The axons of pheromone-sensitive OSNs project to a sexually dimorphic set of glomeruli in the AL known as the macroglomerular complex (MGC). In *H. armigera*, the largest unit of the MGC, the cumulus, receives input from OSNs tuned to Z11-16:AL whereas the two smaller units, dm-a and dm-p are assumed to receive input regarding Z9-16:AL and Z9-14:AL, respectively (Berg et al., 2014). The remaining glomeruli in the AL, ordinary glomeruli (OG), are involved in processing information about non-pheromone odors such as plant odors (kairomones), mechanosensory input, temperature, and CO2 (Han, Hansson, &

Anton, 2005; Hansson & Christensen, 1999; Mizunami, Nishino, & Yokohari, 2016; Zhao et al., 2013b). In male *H. armigera* there is a total of 81 glomeruli in each AL (Zhao et al., 2016). Within the glomeruli, the OSNs form cholinergic, excitatory presynaptic terminals with the principal AL output neurons known as projection neurons (PNs) (see Figure 2B; Figure 3A) (Wilson & Mainen, 2006). The convergence of a large number of OSNs onto relatively few PNs (e.g., in male M. sexta: ~ 255 000 OSNs: ~860 PNs; Homberg, Christensen, & Hildebrand, 1989) serve to (1) increase the signal-to-noise ratio and (2) reduce noise related to external fluctuations in odor concentrations (reviewed by Kay & Stopfer, 2006). PNs can have uni- or multiglomerular arborizations and in turn transmit information to higher brain areas in the protocerebrum through several parallel fiber pathways (discussed below). Most PNs release acetylcholine and excite their target neurons, while a subset of PNs is GABAergic and inhibit postsynaptic neurons.

Within the AL, inhibitory, GABAergic local interneurons (LNs) innervates all or most glomeruli and shape the olfactory processing in the glomeruli through lateral inhibition (Martin et al., 2011). They may also contribute to the synchronous, oscillatory firing activity of PNs (Laurent & Davidowitz, 1994). A fourth type of neuron, centrifugal neurons (CNs), usually have soma located outside of the AL, dendritic ramifications in the protocerebrum and extend synaptic terminal projections into all or most glomeruli in one or both ALs (e.g., see Figure 3B, C) (Anton & Homberg, 1999). CNs constitute a broad range of morphologically and physiologically diverse neurons which may play a role in modulation of the activity of intrinsic AL neurons through the release of neurotransmitters such as serotonin, octopamine, and dopamine (Anton & Homberg, 1999). The precise wiring pattern of CNs to other AL neurons is largely unknown and likely to vary among different types of CNs. However, studies using electron microscopy and pharmacological techniques have demonstrated that one prominent type of CN, the *contralaterally projecting serotonin-immunoreactive deutocerebral* (CSD) neuron (see Figure 3B), has presynaptic connections to PNs and LNs, and additionally receives input from LNs and certain, glomerulus-specific OSNs (Coates et al., 2017; Sun, Tolbert, & Hildebrand, 1993).

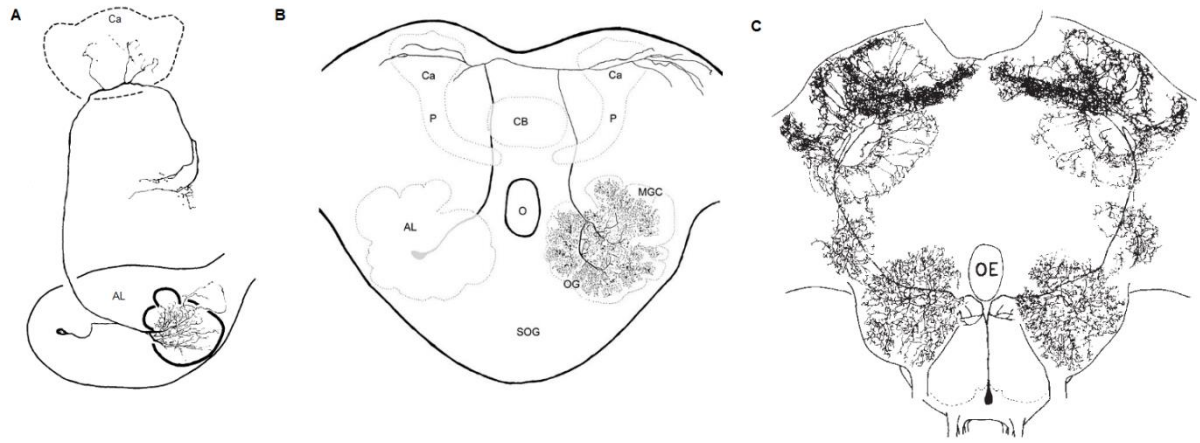

Figure 3. Projection neurons and centrifugal neurons in the insect brain. **(A)** A PN with dendrites in the male-specific MGC projects in the m-ALT and innervates the calyces of the MB and the lateral protocerebrum, in dorsal view. **(B)** The contralaterally projecting, serotonin-immunoreactive deutocerebral neuron, in frontal view. This neuron has its soma located in one AL and innervates the protocerebrum in both hemispheres and the contralateral AL. **(C)** The ventral unpaired median neuron has extensive dendritic ramifications in the protocerebrum and innervates both ALs. The soma is located ventrally, in the gnathal ganglion. AL, antennal lobe; Ca, calyces; CB, central body; MGC, macroglomerular complex; P, pendunculus; O/OE, oesophagus; OG, ordinary glomeruli; SOG, subesophageal ganglion (now referred to as the gnathal ganglion). Modified from Hansson et al. (1994), Zhao & Berg (2009), and Hammer, (1993).

1.2.3 Projection neuron physiology

The morphological and physiological characteristics of PNs have been extensively reported through single-cell electrophysiological recordings in a number of different moth species (*Agrotis segetum*: Hansson, Anton, & Christensen, 1994; Hartlieb, Anton, & Hansson, 1997; *Bombyx mori*: Kanzaki, Soo, Seki, & Wada, 2003; *Helicoverpa assaulta*: Zhao & Berg, 2010; *Heliothis subflexa*: Vickers & Christensen, 2003; Wu, Anton, Löfstedt, & Hansson, 1996; *Heliothis virescens*: Christensen, Mustaparta, & Hildebrand, 1995; *Helicoverpa zea*: Christensen, Mustaparta, & Hildebrand, 1991; *M. sexta*: Christensen & Hildebrand, 1987; Kanzaki, Arbas, Strausfeld, & Hildebrand, 1989; King, Christensen, & Hildebrand, 2000; Kuebler, Olsson, Weniger, & Hansson, 2011; Reisenman, Christensen, Francke, & Hildebrand, 2004; Reisenman, Christensen, & Hildebrand, 2005; *Spodoptera littoralis*: Anton & Hansson, 1995). These studies have largely focused on how male-specific PNs innervating the MGC encode odor identity and concentration, and they have demonstrated considerable diversity in MGC PN response patterns to pheromone components. Some PNs respond selectively only to single components and to a natural blend of the pheromone components ("component-specific), others respond to all pheromone components and the pheromone blend ("generalists"), whereas some respond to either individual pheromone components or the blend, but not both ("blend-specific") (Anton & Hansson, 1995; Christensen &

Hildebrand, 1987; Christensen et al., 1991; Christensen et al., 1995; Hartlieb et al., 1997; Kanzaki et al., 1989; Wu et al., 1996). These studies demonstrate that odor identity can be represented in PNs by using two coding schemes: labeled-line coding, seen in those PNs that respond selectively only to one pheromone component; and across-fiber coding, in which one PN responds to multiple, individual components and/or a blend of pheromone components. Studies have revealed how concentration of stimuli also play important roles in PN response patterns: high pheromone concentrations reduce PN selectivity and increase firing rate (Hartlieb et al., 1997; Kuebler et al., 2011). Furthermore, PNs have different response patterns to odorant stimulation. A common response pattern observed in both OG and MGC PNs in the presence of an odorant, is a rapid, burst of spikes (excitation) followed by suppression of spiking activity (inhibition) (Christensen & Hildebrand, 1987; Kanzaki et al., 2003; Reisenman et al., 2005). Other PNs may respond similarly but without the presence of an inhibitory phase (Christensen et al., 1991), and some PNs generate long trains of spikes which outlasts the length of the stimulus presentation (Kanzaki et al., 1989). Some PNs may also exhibit pure inhibition in response to odorants, in which the firing rate is suppressed during, and for a short time after, stimulus presentation (Zhao et al., 2014). These varied response patterns likely reflect differences in the excitatory and inhibitory connections between OSNs, PNs, and LNs within the AL.

1.2.4 Parallel tracts relay odor information to higher brain areas

In moths, six parallel fiber pathways called antennal-lobe tracts (ALTs) connect the AL with higher brain areas: the medial-ALT (m-ALT), medio-lateral-ALT (ml-ALT), lateral-ALT (l-ALT), dorsal-ALT(d-ALT), dorso-medial-ALT (dm-ALT), and transverse-ALT (t-ALT) (Figure 4) (Homberg, Montague, & Hildebrand, 1988; Ian, Berg, Lillevoll, & Berg, 2016a; Rø, Müller, & Mustaparta, 2007).

The m-ALT is the most prominent ALT (~ 400 PNs in the sphinx moth *M. sexta*) and contains mainly uniglomerular PNs (Homberg et al., 1988). Cell bodies of m-ALT PNs are dispersed in all three cell clusters of the AL: the medial cell cluster (MCC), anterior cell cluster (ACC), and the lateral cell cluster (LCC). From the AL, the m-ALT projects posteriorly along the lateral edge of the central body. The main axon bundle passes anteriorly to the calyces, and several branches extend into, and innervate, the calyces. The m-ALT finally terminates in the LH, AVLP or the SLP.

The majority of ml-ALT PNs (~120 PNs in *M. sexta*) have dendritic ramifications within multiple glomeruli and projects to the LH or larger areas in the lateral and superior

protocerebrum, but usually not the calyces (Homberg et al., 1988; Rø et al., 2007). All ml-ALT somata are located in the LCC. The ml-ALT follows the m-ALT but turns laterally at the anterior, lateral edge of the central body and projects into the LH. Some fibers project posteriorly from the LH and terminate anteriorly to the calyces. Approximately half of the fibers in the ml-ALT are GABAergic and (Berg, Schachtner, & Homberg, 2009; Hoskins, Homberg, Kingan, Christensen, & Hildebrand, 1986).

The l-ALT (~340 PNs in *M. sexta*) projects more ventrally than the m-ALT and ml-ALT and consists of both uni- and multiglomerular PNs with somata in the LCC (Homberg et al., 1988; Rø et al., 2007). The l-ALT turns laterally upon leaving the AL and extends branches into the LH. Additionally, some of the l-ALT PNs project posteriorly from the LH and innervates the calyces, and some projects to the contralateral protocerebrum. Another subset of fibers in the l-ALT targets a separate neuropil structure close to the a-lobe of the MB, called the column (Homberg et al., 1988; Ian et al., 2016a; Ian, Zhao, Lande, & Berg, 2016b; Rø et al., 2007).

The d-ALT has only been reported in the sphinx moth *M. sexta* (Homberg et al., 1988; Hoskins et al., 1986; Kanzaki et al., 1989) and *H. virescens* (Berg et al., 2009), and in *M. sexta* it contains ~50 PNs. Similar to PNs in the ml-ALT, roughly half of the d-ALT PNs are GABAergic (Berg et al., 2009; Hoskins et al., 1986). Interestingly, the dendrites of d-ALT PNs target multiple glomeruli in one AL, whereas their cell bodies are located in the MCC in the contralateral AL. d-ALT fibers project dorso-medially to the l-ALT and innervate the lateral protocerebrum but not the calyces.

The dm-ALT is barely reported. In *M. sexta*, this tract consists of ~16 fibers projecting parallel to the m-ALT, albeit more dorso-medially. The dm-ALT innervates the LH, the inferior median protocerebrum, the lateral accessory lobe (LAL), and regions in the lateral protocerebrum which overlaps with that of some l-ALT PNs (Homberg et al., 1988). The individual dm-ALT PN reported by Rø et al. (2007), having its soma located in the LCC, innervated one single glomerulus extensively and had some additional branches in other parts of the AL. This neuron terminated in the ipsilateral MB and LH.

The t-ALT was first discovered in the fruit fly *Drosophila melanogaster* (Tanaka, Endo, & Ito, 2012a; Tanaka, Suzuki, Dye, Ejima, & Stopfer, 2012b) and recently in *H. virescens* (Ian et al., 2016a; Ian et al., 2016b). It consists of multiglomerular PNs that projects along the m-ALT before turning laterally at the posterior edge of the central body. Ventral to the pedunculus, the t-ALT bifurcates and sends one branch towards the calyces and another to the LH. In *D. melanogaster* the t-ALT also innervates the calyces. Due to the unusual

morphology, the t-ALT may have been characterized as another ALT. For instance, both Homberg et al. (1988) and Rø et al. (2007) likely found t-ALT PNs but classified them as m-ALT PNs (see figure 7C in Homberg et al. (1988) and figure 3F in Rø et al. (2007). In both studies, these PNs were categorized as PIc neurons).

The precise number of ALTs in the insect brains is species-specific, but in most orders of insects, olfactory information is conveyed via the m-ALT, ml-ALT, and l-ALT to the calyces and the lateral protocerebrum (reviewed by Galizia & Rössler, 2010). Furthermore, multiple PN subtypes have been reported in the three classical ALTs in moths (Homberg et al., 1988; Ian et al., 2016b; Rø et al., 2007), and also in t-ALT PNs in *D. melanogaster* (Tanaka et al., 2012a). Despite little knowledge of the d-ALT, dm-ALT, and t-ALT in moths, it is reasonable to expect subtypes in these ALTs. The ubiquitous presence of multiple, parallel ALTs, which differ from another in glomerular innervation pattern, output regions in the protocerebrum, and neurotransmitter content, suggests that they possess different functional roles in olfactory processing (Galizia & Rössler, 2010). A similar structural and functional organization is seen in the mammalian visual system, where separate, parallel pathways mediate various features of visual stimuli (Livingstone & Hubel, 1988; reviewed by Nassi & Callaway, 2009). For instance, multiglomerular PNs in *D. melanogaster* exhibit a broader response profile to odorants than uniglomerular PNs (Wang et al., 2014). Differences are also seen in neural levels further downstream. The calyces are predominantly innervated by PNs in the m-ALT, and more sparsely by neurons in the l-ALT, t-ALT, and dm-ALT. This suggests that odor information conveyed in these ALTs play a role in learned, odor-evoked behaviors. Contrary, PNs in the ml-ALT and d-ALT may be more involved in innate behavioral responses, as they projects primarily to the LH and other regions in the lateral protocerebrum. In addition to anatomical differences in input and output organization, the ml-ALT and d-ALT are also functionally separated from the other ALTs due to the release of GABA. In *D. melanogaster*, inhibitory PNs have been shown to mediate odor attraction (Strutz et al., 2014), and enhance odor discrimination by selectively inhibiting the activity of low-frequency, but not high-frequency, excitatory PNs in the LH (Parnas, Lin, Huetteroth, & Miesenböck, 2013).

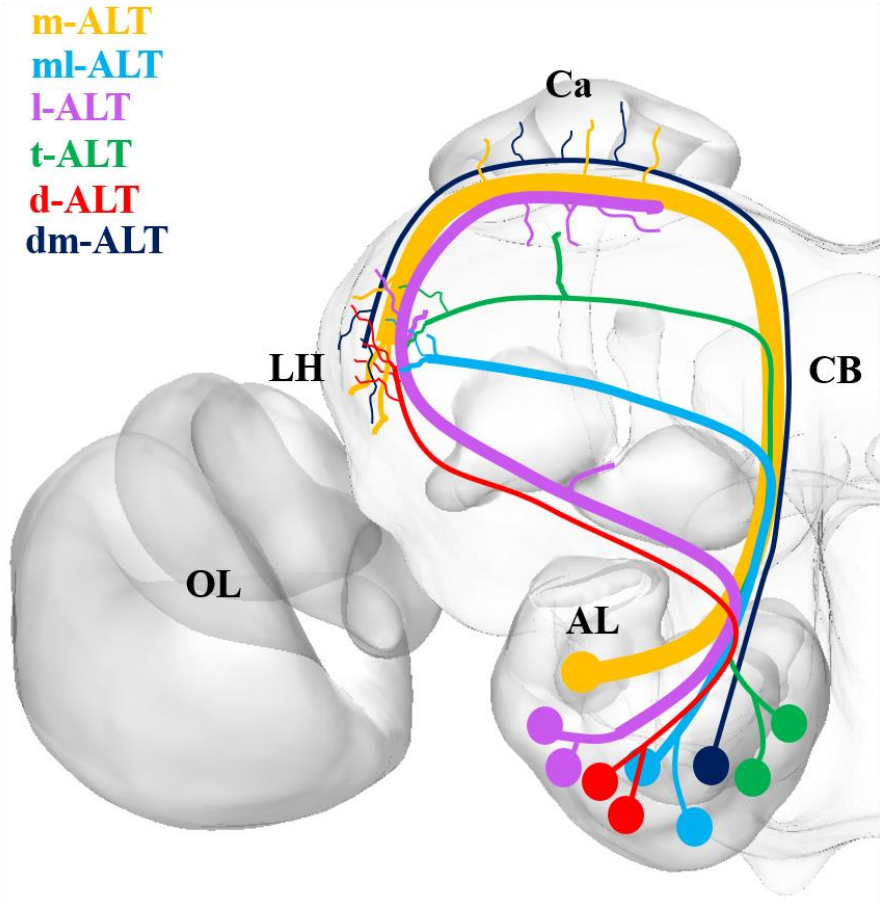

Figure 4. Schematic representation of the six parallel ALTs reported in moths, in dorsal view. Note that while all tracts terminate in the lateral protocerebrum, only the m-ALT, l-ALT, and t-ALT innervates the calyces. Tracts that have multiglomerular arborizations in the AL are assigned by two 'glomeruli' in the AL. Uniglomerular tracts are indicated by a single glomerulus. The number of neurons in each tract is roughly indicated by the width of the tract. AL, antennal lobe; Ca, calyces of the mushroom body; CB, central body; LH, lateral horn; OL, optic lobe.

1.2.5 Olfactory processing in higher brain areas

With some exceptions, all ALTs project to two regions in the protocerebrum: the calyces of the mushroom bodies and the lateral protocerebrum. In heliothine moths, the mushroom bodies (MB) consist of the calyces, the pedunculus, and the various lobes (See Figure 3B, 5A) (Rø et al., 2007). Within the calyces, terminal output synapses from neurons involved in olfactory, visual, gustatory, and mechanosensory information processing contact the dendrites of intrinsic MB cells known as Kenyon cells (Stopfer, 2014). Chemical ablation of the MB in combination with behavioral assays have implied that this structure is critical for associative olfactory learning (Connolly et al., 1996; de Belle & Heisenberg, 1994).

The lateral protocerebrum is a large neuropil consisting of the posterior lateral protocerebrum (PLP), posterior ventro-lateral protocerebrum (PVLP), anterior ventro-lateral protocerebrum (AVLP), LH, and superior lateral protocerebrum (SLP) (see Figure 5).

Contrary to the MB, regions of the lateral protocerebrum are associated with experience-independent behaviors, such as walking, flying, and courtship (de Belle & Heisenberg, 1994; Heimbeck, Bugnon, Gendre, Keller, & Stocker, 2001; McBride et al., 1999). Projection neurons target four regions in the lateral protocerebrum: the LH, AVLP, SLP, and the column (Homberg et al., 1988; Rø et al., 2007; Seki, Aonuma, & Kanzaki, 2005; Zhao et al., 2014). Projection neurons which innervate ordinary glomeruli terminate mainly in the LH, while PNs with dendrites in the MGC innervate more anterior regions of the lateral protocerebrum, notably the AVLP and SLP (previously referred to as the delta area of the inferior lateral protocerebrum), and the column. A similar division of pheromone and non-pheromone processing areas is also seen in *D. melanogaster* (Jefferis et al., 2007). Thus, pheromone and non-pheromone odor information is processed in different regions of the lateral protocerebrum. Additionally, the LH itself appear to be further partitioned into different functional areas: in *D. melanogaster*, spatially separated areas of the LH encode odors of opposite hedonic valence (attraction/avoidance) (Min, Ai, Shin, & Suh, 2013; Strutz et al., 2014). Therefore, although the lateral protocerebrum is largely anatomically unstructured, it is functionally organized into regions involved in distinct olfactory processes.

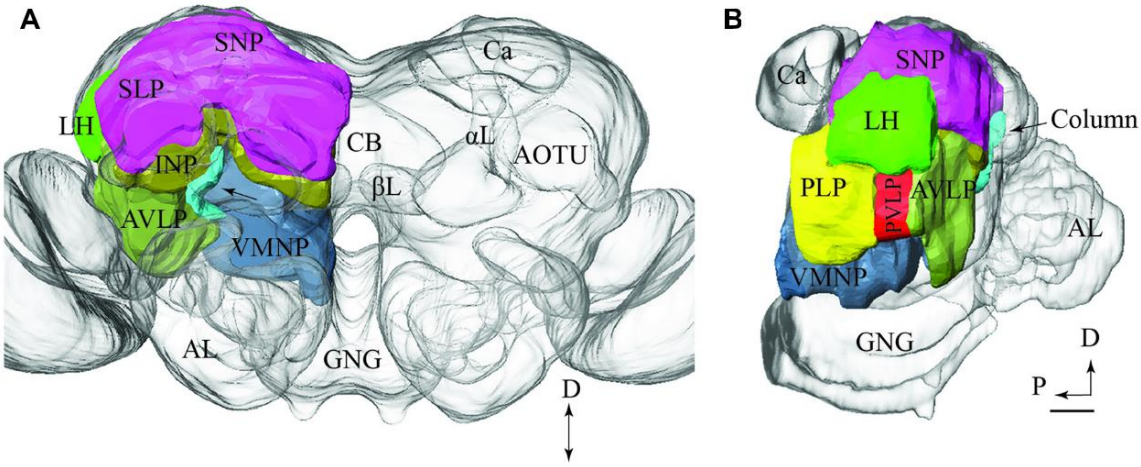

Figure 5. Model brain indicating various neuropils in the protocerebrum. **(A)** Frontal view, slightly tilted dorsally. **(B)** Sagittal view. Arrows point to the column. αL, alpha-lobe; AL, antennal lobe; AOTU, anterior optic tubercle; AVLP, anterior ventro-lateral protocerebrum; Ca, calyces of the mushroom body; CB, central body; βL, beta-lobe; LH, lateral horn; GNG, gnathal ganglion; INP, inferior neuropils; PLP, posterior lateral protocerebrum; PVLP, posterior ventro-lateral protocerebrum; SLP, superior lateral protocerebrum; SNP, superior neuropil; VMNP, ventro-medial neuropil. Scale bars: 50µm. Modified from Ian et al. (2016b).

1.2.6 Modulation of odor processing in the antennal lobe by centrifugal neurons

Centrifugal neurons modulate neuronal activity in the primary olfactory processing center in both vertebrates and invertebrates (Wilson & Mainen, 2006). In mammals, for instance, serotonergic neurons projecting from the raphe nuclei in the brain stem provide top-down modulation of mitral and tufted cells (Kapoor, Provost, Agarwal, & Murthy, 2016). CNs in insects are assumed to modulate olfactory processing in the AL based on input from other sensory modalities (Zhao, Pfuhl, Surlykke, Tro, & Berg, 2013a), the general state of the animal (reviewed by Lizbinski & Dacks, 2018), or circadian rhythms (reviewed by Kloppenburg & Mercer, 2008). In *D. melanogaster*, hunger, reproductive state, and sickness may alter sensory thresholds and behavioral responses through the action of modulatory neurons (reviewed by Sayin, Boehm, Kobler, De Backer, & Grunwald Kadow, 2018). In the honeybee, an octopaminergic CN known as the ventral unpaired median (VUM) neuron have extensive innervation throughout the ALs and the protocerebrum, and encodes the unconditioned stimulus in appetitive, associative olfactory learning (see Figure 3C) (Hammer, 1993; Hammer & Menzel, 1998).

The morphology and physiology of the CSD neuron have been studied in several insect species (D. melanogaster: Coates et al., 2017; Bombyx mori: Hill, Iwano, Gatellier, & Kanzaki, 2002; M. sexta: Kent, Hoskins, & Hildebrand, 1987; Periplaneta americana: Salecker & Distler, 1990; D. melanogaster: Zhang & Gaudry, 2016; Helicoverpa assaulta: Zhao & Berg, 2009). The CSD neuron is present in most holometabolous insect orders, albeit with some morphological differences (reviewed by Dacks, Christensen, & Hildebrand, 2006). The soma of the CSD neurons is located in the postero-ventral region of one AL, while its neurites arborize within every glomeruli in the contralateral AL (see Figure 3B). In the protocerebrum, dendritic processes branch in the superior and lateral protocerebrum, in addition to the calyces. Each insect brain contains two CSD neurons which mirror each other in terms of dendritic arborizations, soma location, and terminal projection fields in the AL. Little is known about the physiological responses of the CSD neuron to odorants and how it influences AL processing. Previous studies of CSD neuron physiology in moths have observed mechanosensory-like excitatory responses (Hill et al., 2002; Zhao & Berg, 2009), whereas in *D. melanogaster* a wide range of odorants, including pheromones, elicits inhibition (Zhang & Gaudry, 2016). This effect is likely mediated by inhibitory LNs. One exception is ammonia, which induces an increase in spiking activity. Other lines of studies have suggested that CSD neurons regulate sensitivity to sex pheromones. Bath application of serotonin in the AL of *M. sexta* increases MGC PN excitability and responsiveness to sex pheromones, partly

caused by reduction in K^+ currents (Kloppenburg, Ferns, & Mercer, 1999). Similar bath application in the moth *Bombyx mori* elicits increased behavioral sensitivity to pheromones (Gatellier, Nagao, & Kanzaki, 2004). This effect was shown to be concentration-dependent: high concentration of serotonin decreased behavioral sensitivity. As the level of serotonin fluctuates throughout the day and peaks when the moths are most active, CSD neurons have been suggested to regulate AL neurons' sensitivity to pheromones in accordance with circadian rhythms (Kloppenburg & Mercer, 2008). However, a recent study in *D. melanogaster* reported contradictory results, as PNs' response to pheromones increased when postsynaptic serotonin receptors were blocked, and conversely, PN response decreased when presynaptic serotonin reuptake transporters were blocked (Zhang & Gaudry, 2016). Furthermore, the same study demonstrated that optogenetic stimulation of the CSD neuron did not modulate the sensitivity of AL neurons to pheromones. Thus, the exact function of serotonergic modulation by the CSD neuron is still not determined.

1.3 Current knowledge gaps and aims of the study

The last decades have accumulated a considerable amount of knowledge of the morphological and physiological characteristics of projection neurons in the m-ALT. However, the morphology and functional role of neurons in the other ALTs remain poorly understood. Similar to the visual system, the parallel organization of the olfactory system suggests that the various pathways perform distinct functions in olfactory processing (Galizia & Rössler, 2010). Even less is known about the centrifugal neurons that provide input to the AL from higher brain areas. These neurons are morphologically diverse and may modulate olfactory processing in different ways depending on their dendritic ramifications in the brain and neurotransmitter content. Although recent studies of heliothine moths have begun to unravel the structure and function of the parallel ALTs (Ian et al., 2016a; Ian et al., 2016b), more data on the anatomy and physiology of individual PNs confined to the different tracts and centrifugal neuron is needed. A better understanding of the structure-function relationship of projection neurons and centrifugal neurons in the insect brain should help us understand the general principles of how the olfactory system encodes, process, and represent odor information our

The current study aims to investigate the morphological features projection neurons and centrifugal neurons in *H. armigera*, and to examine the physiological responses of these neurons to pheromone- and plant odorant, using intracellular recording and iontophoretic staining in combination with confocal microscopy. Specifically, we will study projection

neurons confined to the various ALTs, and see whether the response selectivity (broad or narrow tuning) to odors can be correlated with morphological features and/or which tract they project in. Furthermore, we will investigate the compartmentalized subsystem devoted to processing of pheromone information, and see how this system is different from non-pheromone olfactory systems in terms of structure and function. Regarding centrifugal neurons, we aim to corroborate and expand on the previous knowledge on the morphological and physiological properties of these neurons, and, if possible, gain insight into their role in olfactory processing.

2. Method

2.1 Insect preparation

Male pupae of the cotton bollworm *H. Armigera* (Lepidoptera: Noctuidae) from China (provided by Henan Jiyuan Baiyun Industry Co., Ltd) were kept in climate chambers at 23-25°C at 70% humidity in a phase-shifted day-night cycle (14h light, 10h dark). Half of the insects were kept in a small rectangular container and upon hatching transferred into cylindrical Plexiglas containers (diameter = 12.5 cm, height = 20 cm), while the other half were kept in a larger cylindrical container (diameter = 29 cm, height = 40 cm) during both pupae and imago phase. All moths had ad libitum access to a 10% sucrose solution. Carefully selected, healthy adult moths (as guided by visual inspection of wings and antennae), one- to six-days post eclosion, were used for intracellular recordings.

In preparation for intracellular recordings, a moth was stored for 10-20 minutes at 4°C for sedation and placed in a 50-1000 µl plastic pipette to restrain movements. The tip of the pipette had been cut off beforehand to expose the moth head and antennae. The head capsule was immobilized by adding a layer of utility wax (Kerr Corporation, Romulus, MI, USA). The specimen was then placed under a stereomicroscope (Leica) and a small piece of paper was gently rubbed against the head cuticle to remove cephalic scales. The head cuticle was cut open using a razor blade and the sheath encapsulating the brain was gently removed with fine forceps. Next, the antennal muscles surrounding the antennal nerve were cut to reduce antennal movements. Ringer's solution (in mM: 150 NaCl, 3 CaCl2, 2 KCl, 25 sucrose, and 10 N-tris (hydroxymethyl)-methyl-2-amino-ethanesulfonic acid, pH 6.9) was applied continuously to prevent desiccation of the brain. After intracellular recording and staining, the preparation was kept overnight at 4°C to allow the dye to be transported within the recorded neuron. The following the day the brain was dissected from the head capsule and stored in 4% paraformaldehyde (Roti-histofix 4%, Carl Roth GmbH, Karlsruhe, Germany) for 1h in room temperature. Subsequently, the brain was dehydrated in an increasing ethanol series (50%, 70%, 90%, 96%, 2 x 100%) for 10 minutes each before it was placed in methyl salicylate (methyl 2-hydroxybenzonate) and stored at 4°C in darkness to prevent photobleaching of the fluorescent dye. Prior to confocal microscopy, the brain was mounted in an aluminum plate in methyl salicylate and covered by decker glass plates.

2.2 Odor stimulation

The odor stimuli used in this study consisted of separate presentation of the primary (Z11-16:AL) and secondary (Z9-16:AL) pheromone component; a 95:5 ratio blend of the primary and secondary component; the behavioral antagonistic, interspecific component (Z9-14:AL; and extracts from sunflower headspace. Sunflower headspace contains multiple odorant components which activates OSNs in *H. armigera* (Røstelien et al., 2005). Except from sunflower headspace extracts, all stimuli was diluted in hexane to reach a concentration of 50 ng/100 µl. Hexane served as the control stimulus. 20-µl of each stimuli including control was applied onto a separate filter paper, which briefly was air-dried before it was placed into a marked glass cartridge. Between the experiments, the stimuli was stored at -18°C.

The odor delivery system consisted of two glass cartridges (ID: 0.4 cm) positioned side by side, both pointed towards the antennae, at a distance of ~1.5cm from the antennae. One cartridge was filled with a clean filter paper and applied a constant stream of air (500ml/min) onto the antennae. The other cartridge was replaceable and allowed for manual switching of the cartridges containing the various stimuli. Presentation of the stimuli was initiated by a command in the software Spike2 (version 6.18, Cambridge Electronics Design), which directed the airflow from the cartridge with the clean filter paper into the cartridge containing the stimuli by a valve system for 400ms. The odor stimuli was renewed regularly every 1-2 week during the experimental phase.

2.3 Intracellular recording and staining

Glass microelectrodes used for intracellular recording were pulled from borosilicate capillaries (Hilgenberg, Germany; OD: 1 mm, ID: 0.75 mm) using a horizontal P-97 Flaming/Brown Pipette Puller (Sutter Instruments Inc., USA) and backfilled with the fluorescent dye Micro-Ruby (dextran, tetramethylrhodamine with biotin, 3000MW, Life Technologies, USA) and 0.2 M potassium acetate. The recording electrode had a resistance of 40-140 MΩ in Ringer's solution prior to entering the neural tissue. A micromanipulator (Leica) was used to lower the microelectrode into the brain dorsally, aimed towards either the lateral or the postero-medial area of one AL, to target either the MGC or the large-diameter fibers containing PN axons. A chloridized silver wire serving as the reference electrode was inserted into the mouth muscle tissues located anteriorly to the brain. If a stable contact with a neuron could not be established within 30 minutes and/or the microelectrode broke (assessed by checking if resistance dropped below 30 MΩ) the remaining AL was used. The recording

and reference electrode were connected to a headstage which relayed neuronal spike signals into an amplifier (Axoprobe 1A, Axon Instruments). The signals were then monitored continuously visually on an oscilloscope and auditory on a loudspeaker. The spike data was stored and analyzed by Spike2. The sampling rate was 1000Hz. After recording neuronal spiking activity, the neurons were iontophoretically stained by injecting 1.5-3.0 nA depolarizing current pulses of 200 ms duration at 1 Hz for 5-15 minutes through the recording electrode.

2.4 Confocal laser scanning microscopy

Whole mounted preparations went through a brief check in a light microscope (Leica, DMC 4500) before they were scanned in a confocal microscope (Zeiss, LSM 800, Jena, Germany) to produce serial scans. Two different objectives were used: a 10x water objective (C-achroplan, 10x/0.45W) for overview images and a 20x air (Pan Neofluar 20x/0.5 NA) for detailed images. A 543-nm helium laser (HeNe1) was used to excite neurons labeled with Micro-ruby (EXmax 555, EMmax 580) while a 488-nm argon laser was used to provide background autofluorescence, illuminating the brain in its entirety. Each scanning frame had a diameter of 10 µm using the 10x objective or 2 µm if the 20x objective was used. The pinhole size was 1 airy unit and image resolution was 1024 x 1024 pixels. The resulting scans was acquired and processed in Zen2 software (blue edition, Carl Zeiss Microscopy, GmbH, Jena, Germany).

2.5 Data analysis

With the exception of a CN, only successfully stained individual neurons were used in analyses of spike data (or, in some cases, 2-3 stained neurons that all belonged to the same ALT). In all spike trains included in the analysis, stimuli presentations was separated by minimum 10s to ensure that eventual neuronal responses from one stimulus trial did not affect the subsequent trial. Furthermore, spike trains had to include the control stimulus to be eligible for analyses. All spike trains included in data analyses went through spike sorting to ensure the match between recorded spike and stained neuron. To study odor-evoked neuronal responses, segments of the spike train lasting 2500ms (1000 ms pre-stimulation, 1500 ms post-stimulation) were analyzed (see Figure 6). The neuronal responses was quantified and visualized by creating color- and response plots, and PSTHs.

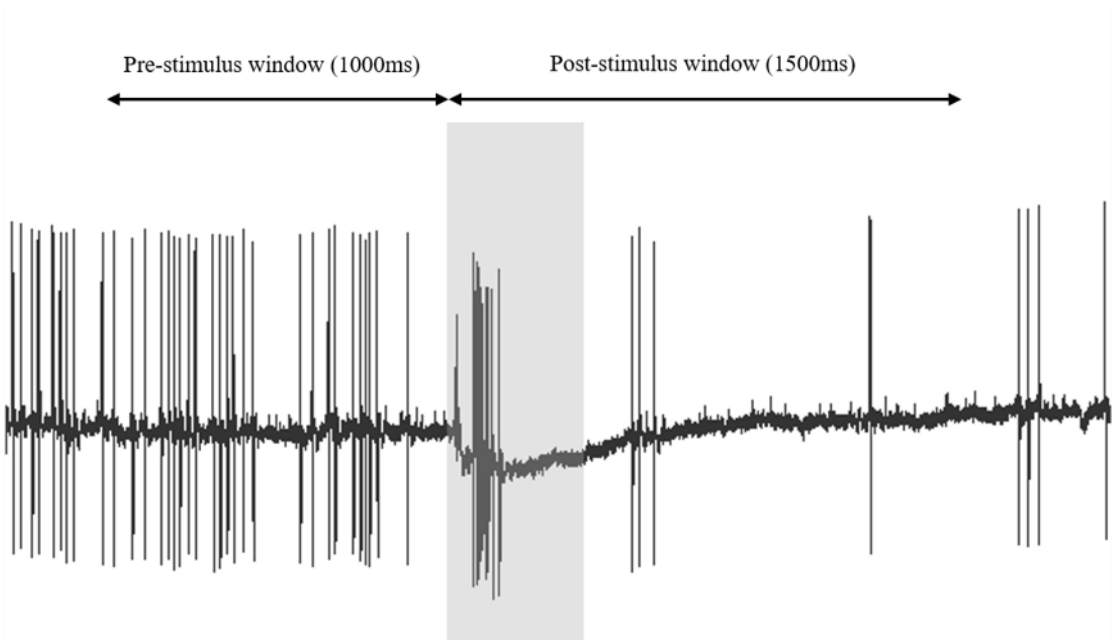

Figure 6. Segments of the spike train that were subjected to data analysis. Stimulus duration indicated by the grey transparent bar, 400ms. Spiking activity from the 1000ms preceding stimulus onset was compared with the spiking activity occurring in the 1500ms following stimulus onset.

2.5.1 Spike sorting

Spike sorting was performed in Spike2, which generates action potential waveform templates based on the shape and form of action potentials that occurred during the intracellular recording. To generate accurate waveform templates, (1) an amplitude threshold was set and (2) the onset and offset of the action potentials was determined, through visual inspection of the raw data. The amplitude threshold ensured that Spike2 only detected and classified action potentials of a given amplitude and not minor fluctuations in the raw data, whereas the onset and offset of action potentials was set to avoid inclusion of multiple spikes in a waveform template. Spike2 then assigned each action potential to a specific waveform template and specified time of occurrence of each spike. The raw data was thoroughly inspected to optimize the detection and classification of action potentials. If Spike2 generated several waveform templates, indicating that the recorded spike train included waveforms from two or more neurons, the average shape and duration of each waveform template was examined. If the general shape, amplitude and full width at half maximum (FWHM) of the different waveform templates did not significantly differ, they were assumed to originate from the same neuron. To further establish that spike trains originated from one neuron, only spike trains belonging to preparations containing one individually stained neuron were analyzed (some exception were made, see Data analysis).

2.5.2 Quantification and visualization of physiological responses

Peri-stimulus time histograms (PSTHs) displaying the number of spikes per second were created in Spike2. To further quantify the odor-evoked responses a modified procedure of that outlined in Reisenman, Dacks, and Hildebrand (2011) was followed. First, the instantaneous spiking frequency (ISF) for each spike during the pre- and post-stimulus window was calculated by the formula provided by Jarriault, Gadenne, Rospars, and Anton (2009):

$ISF = 1/(t_i - t_{i-1})$,

where *t* denotes the spike time of the *i*th spike. Then, the statistical significant number of ISFs in response to an odorant-stimulus was determined by calculating an upper and lower threshold around the mean ISF in the pre-stimulus window:

A = mean $_{ISFPRE}$ + (standard deviation - mean $_{ISFPRE}$ * 1.96)
B = mean $_{ISFPRE}$ - (standard deviation - mean $_{ISFPRE}$ * 1.96)

These were calculated separately for each stimulus presentation. The spikes in the post-stimulus window whose ISF were higher or lower than the values obtained in A and B, were considered to be the statistically significant number of positive or negative spikes, respectively.

If statistically significant ISFs above A (positive ISFs) and below B (negative ISFs) both were present in the post-stimulus window, the number of negative ISFs was subtracted from the positive ISFs to obtain the overall positive or negative response. This procedure was repeated for all trials which presented the same stimulus in one neuron. They were then added together to get a total number of positive or negative ISFs in response to an odorant. To determine whether a neuron had an excitatory, inhibitory, or no response to an odorant stimulus, two additional values were calculated:

C = mean number of significant ISFs evoked by control stimulus + (total number of positive ISFs evoked by control *$SE_{TOTAL\ A}$)

D = mean number of significant ISFs evoked by control stimulus - (total number of negative ISFs evoked by control*$SE_{TOTAL\ B}$)

Here, $SE_{TOTAL\ A}$/$SE_{TOTAL\ B}$ refer to the standard error of all A and B values calculated for each presentation of a given stimulus. A response was considered excitatory if the mean number of ISFs evoked by a stimulus was larger than C. If the mean number of ISFs was below D it was classified as an inhibitory response. If the mean number of ISFs fell between C and D, it was classified as no response. Three modifications had to be made to improve the subsequent response classification: First, as observed in Reisenman et al. (2011), excitatory responses were correctly classified but the procedure frequently failed to detect putative inhibitory responses. Thus, for these responses, the total number of ISFs in the pre-stimulus window was subtracted from the total number of ISFs in the post-stimulus window. The post-stimulus window was set to 1000ms as the inhibitory response often was short-lasted and spiking activity resumed quickly after stimulus offset. Second, some trials contained no spikes, and thus no ISFs, in the pre-stimulus window, resulting in the erroneous calculation of the number of statistically significant ISFs as zero. In these cases, all spikes in the post-stimulus window was classified as statistically significant positive ISFs. Third, responses were often misclassified as inhibitory, because the lower threshold (D-value) was set too high: whenever the control stimulus elicited no negative ISFs, the D-value was set equal to the mean number of ISFs evoked by the control stimulus. Thus, a response to an odorant consisting of a single, positive ISF could be classified as inhibitory if the mean number of ISFs evoked by the control stimulus was > 1. To resolve this, the lower threshold (D-value) was set equal to the distance between the mean and the upper threshold (C-value), but in opposite direction. The procedure correctly classified 74.4% of the responses, as compared to visual inspection of the raw data. In the few cases were the classification appeared to be wrong, a visual inspection had the final word. All quantification analyses was made in Matlab (Mathworks, Inc) using a custom script.

2.6 Terminology

To describe the different antennal-lobe tracts and regions terminology from Ito et al. (2014) was adopted. This paper outlines a common terminology of areas in the insect brain using the *D. Melanogaster* as the reference model, developed by a group of leading researchers on invertebrates. To describe the mushroom bodies, including the calyces,

pedunculus, and the various lobes, terminology was adopted from Rø et al. (2007) who conducted an anatomical study of these structures in *H. virescens*.

2.7 Ethical considerations

Insects belonging to the lepidopteran species are not included in the *Regulation for use of animals in research trials* (Forskrift om bruk av dyr i forsøk). Nonetheless, care was taken to provide an ethical treatment of the experimental subjects. The moths were housed in Plexiglas containers in climate chambers which provided natural temperature and light environment. The moths were cared for every day by changing soiled tissue papers (which covered the floor and walls of the container) and ensuring that they had *at libitum* access to sucrose water. To avoid space-related stress, no more than 8 moths were housed in one container.

3. Results

Through intracellular recordings and iontophoretic staining, we investigated the morphological characteristics and physiological responses to pheromone and plant odors in two principal types of AL neurons: projection neurons and centrifugal neurons. A total of 156 moths was used in this study, of which intracellular recordings were made in 126 neurons. 25 neurons were successfully stained according to the criteria stated in the Method section (see 2.5 data analysis). Three extra neurons were also included for data analysis, among them 2 PNs were collected by post doc Xi Chu and one CN by Ph.d student Jonas Hansen. In addition, three preparations without electrophysiological examination were included only in the anatomical analysis. The structure and function of 28 neurons (PN n = 25; CN n = 3) was analyzed, in addition to morphological analyses of three neurons (PN n = 2; CN n = 1). The morphological characteristics of all 31 neurons are displayed in Table 1, whereas the physiological data of 28 neurons are reported in the section 3.3.

3.1 Projection neuron morphology

3.1.1 m-ALT projection neurons

Eighteen m-ALT PNs were successfully stained in this study (see Figure 7). These neurons projected posteriorly from the AL and passed the lateral edge of the central body before turning laterally and innervated the calyces and lateral protocerebrum. 11 neurons in the m-ALT were classified as Pm_a_OG neurons, and 4 as Pm_a_MGC neurons, in accordance with the subtypes presented in Homberg et al. (1988). Three m-ALT neurons could not be classified into a distinct subtype due to weak staining of the dendritic area in the AL and terminal projection field in the LH. This type of PNs have been described in *H. virescens* and *Helicoverpa assulta* (Zhao & Berg, 2010; Zhao et al., 2014), and morphological structures are rather similar across the species.

All Pm_a_OG neurons innervated a single, ordinary glomerulus, had the soma in the MCC or LCC, and projected to the LH (see Figure 7A, B; Appendix Figure 1). As reported by Homberg et al. (1988), there was a certain geometrical relationship between soma location and innervated glomerulus. Projection neurons generally innervated a closely located glomerulus. One Pm_a_OG (#1) neuron extended a side branch into an adjacent glomerulus, in addition to the primary innervated glomerulus (see arrow in appendix figure 1D). This side branch parted from the main dendrite just after the main dendrite exited the glomerulus, and innervated an adjacent glomerulus. Similar innervation pattern has been observed by

Homberg et al. (1988) and Rø et al. (2007). In the protocerebrum, the main axon of Pm_a_OG neurons passed anteriorly to the calyces, and sent 3-5 branches into the calyces. Here, they formed numerous varicosities (see dashed circle in Figure 7B). Such enlargements in segments of the neurites are generally interpreted as presynaptic boutons (Cardona et al., 2010). Then, the axon continued antero-laterally and terminated in the LH. Several side branches extended from the main axon, each with a large number of blebs (see dashed circle in Figure 7A). A few Pm_a_OG neurons also extended some branches from the LH anteriorly into the posterior ventrolateral protocerebrum (PVLP).

Table 1

Total overview of the morphological characteristics of labeled projection neurons and centrifugal neurons

Cell ID	Neuron type	ALTs	Subtype	Somata location	Dendritic arborization	Terminal projections
1	PN	m-ALT	Pm_a_OG	LCC	AL (UG)	Ca; LH
2	PN	m-ALT	Pm_a_OG	MCC	-	Ca; LH
3	PN	m-ALT	-	MCC	-	Ca; LH
4	PN	m-ALT	Pm_a_OG	MCC	AL (UG)	Ca; LH
5	PN	m-ALT	Pm_a_OG	MCC	AL (UG)	Ca; LH
6	PN	m-ALT	Pm_a_OG	MCC	AL (UG)	Ca; LH
7	PN	m-ALT	Pm_a_OG	-	AL (UG)	Ca; LH
8	**PN**	**m-ALT**	**Pm_a_MGC**	MCC	AL (UG)	Ca; PVLP; AVLP;SLP
9	**PN**	**m-ALT**	**Pm_a_MGC**	MCC	-	Ca; LH; AVLP
10	**PN**	**m-ALT**	**Pm_a_MGC**	MCC	-	Ca; LH; PVLP; SLP
11	PN	m-ALT	Pm_a_OG	-	-	Ca; LH; PVLP
12	**PN**	**m-ALT**	**Pm_a_MGC**	MCC	AL (UG)	Ca; PVLP; AVLP; SLP
13	PN	m-ALT	Pm_a_OG	MCC	AL (UG)	Ca; LH
14	PN	m-ALT	Pm_a_OG	MCC	AL (UG)	Ca; LH
15	PN	m-ALT	-	-	-	Ca; LH
16	PN	m-ALT	Pm_a_OG	MCC	AL (UG)	Ca; LH
17	PN	m-ALT	-	MCC	-	Ca; LH; SLP
18	PN	m-ALT	Pm_a_OG	MCC	-	Ca; LH
19	**PN**	**ml-ALT**	**Pml_a_MGC**	LCC	AL(MG)	AVLP
20*	**PN**	**ml-ALT**	**Pml_a_MGC**	LCC	AL (MG)	AVLP
21	PN	ml-ALT	Pml_c_OG	LCC	AL (UG)	LH; PLP; SLP
22	PN	l-ALT	-	-	-	LH
23	PN	l-ALT	-	LCC	AL (MG)	-
24*	**PN**	**l-ALT**	**Pl_a_MGC**	LCC	AL (UG)	AVLP; column
25	PN	l-ALT	Pl_b_OG	LCC	AL (MG)	AVLP
26**	PN	t-ALT	Pt_b	LCC	AL(MG)	Ca; LH; PLP
27**	PN	d-ALT	Pd	Contralateral MCC	AL (MG)	Ca; LH; PLP; PVLP; AVLP; SLP
28**	CN		BPC	~Ca	SMP; SIP	Both ALs
29	CN		BPC	~Ca	SMP; SIP	Both ALs
30	CN		CSD	LCC	Ca; CB; LH; SLP	Contralateral AL
31	CN		CSD	LCC	Ca; CB; LH; SLP	Contralateral AL

Note. Bold font indicates that projection neurons innervate the macroglomerular complex (MCG). AL, antennal lobe; AVLP, anterior ventro-lateral protocerebrum; Ca, calyx; CN, centrifugal neuron; CB, central body; CSD, contralaterally projecting, serotonin-immunoreactive deutocerebral neuron; BPC, bilateral paired centrifugal neuron; LCC, lateral cell cluster; LH, lateral horn; MCC, medial cell cluster; MG, multiglomerular; OG, ordinary glomeruli; PN, projection neuron; PLP, posterior lateral protocerebrum; PVLP, posterior ventro-lateral protocerebrum; SIP, superior intermediate protocerebrum; SLP, superior lateral protocerebrum; SMP, superior medial protocerebrum; UG, uniglomerular. *Neurons were provided by Xi Chu or Jonas Hansen. ** Neurons were not included in physiological analyses.

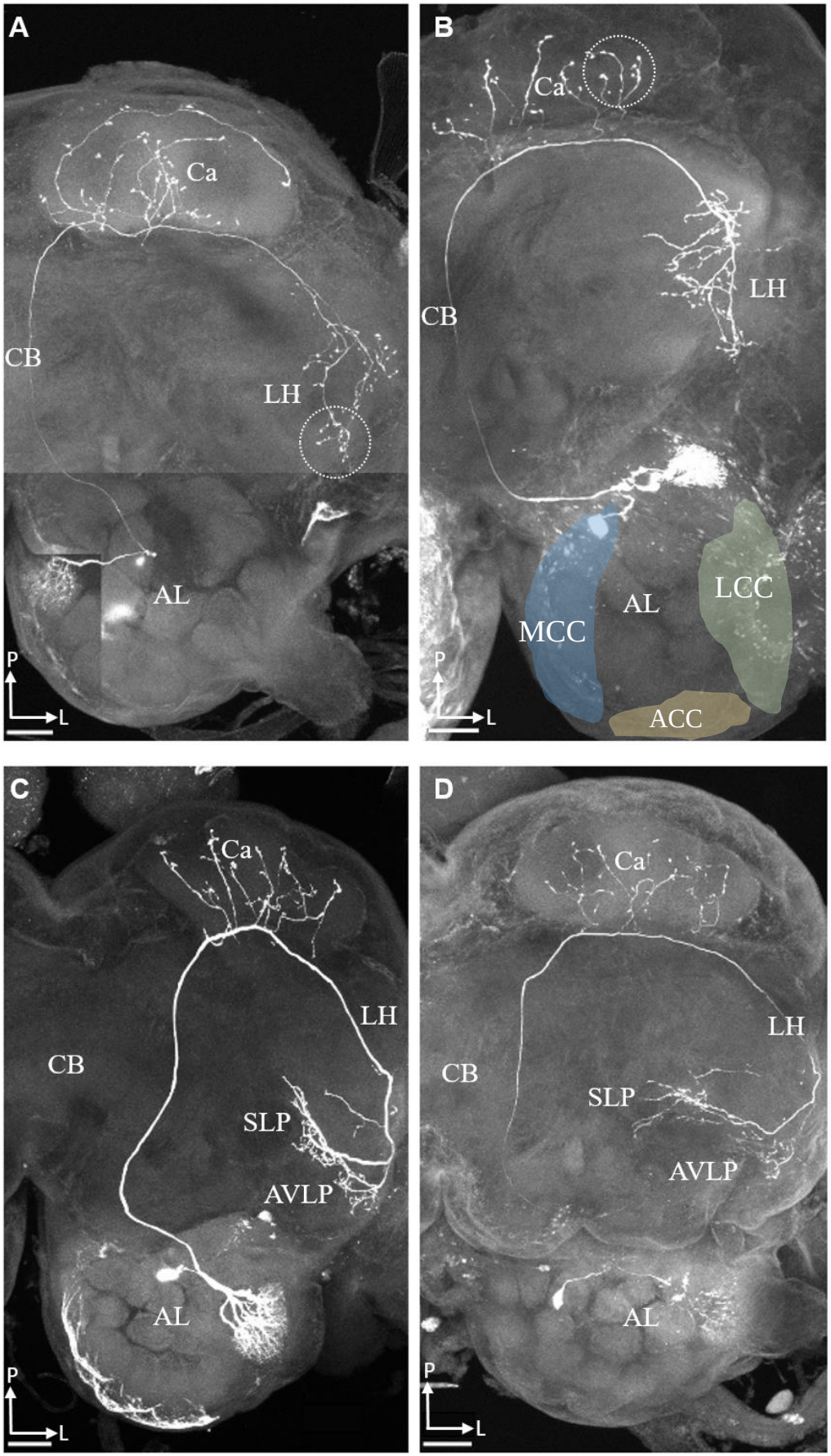

Figure 7. Confocal images of four medial antennal lobe tract (m-ALT) projection neurons (PNs), in dorsal view. **(A-B)** Each PNs (#13, 6) in the m-ALT innervated a single, ordinary glomerulus (OG) in the AL. These PNs projected to the calyces (Ca) and the lateral horn (LH). Note the many varicosities

on the branches in the protocerebrum (indicated in dashed circles). **(C-D)** PNs (#7, 12) in the m-ALT innervating the male-specific macroglomerular complex (MGC). Both neurons innervated the cumulus unit. Note that these neurons have more sparse innervation of the calyces than OG PNs, and terminate in the anterior ventrolateral protocerebrum (AVLP) and superior lateral protocerebrum (SLP). The soma of all four neurons are located in the medial cell cluster (MCC). ACC, anterior cell cluster; CB, central body; LCC, lateral cell cluster. Scale bars: 50 µm.

Medial-tract PNs with dendrites in the male-specific glomeruli, the MGC, were observed in four preparations (two are shown in Figure 7C, D). From the AL, Pm_a_MGC neurons followed the same pathway as the previously described Pm_a_OG neurons, but had less extensive innervation of the calyces and projected to more anterior regions of the lateral protocerebrum. The cell body of all Pm_a_MGC PNs was located in the MCC. Two preparations contained individual PNs which innervated the cumulus unit of the MGC. One unshown preparation contained two MGC PNs, one innervating the cumulus and one innervating the dm-p unit. Identification of glomerular innervation could not be determined for the fourth preparation, unshown data. Compared to Pm_a_OG neurons, the Pm_a_MGC PNs had fewer branches and smaller varicosities in the calyces and projected to anterior regions of the lateral protocerebrum, including the PVLP and anterior ventro-lateral protocerebrum (AVLP), were a few, short fibers were observed extending from the main branches. From these areas, the neurons turned dorso-medially and projected one or two branches into the superior lateral protocerebrum (SLP).

3.1.2 ml-ALT projection neurons

Three ml-ALT PNs with soma located in the LCC were reported in this study (see Figure 8; Appendix Figure 2B). The main axon of neurons in the ml-ALT exited the AL along with the m-ALT axon bundle but diverged anterior to the lateral edge of the central body. From there, they projected directly to the lateral protocerebrum and did not innervate the calyces. Two ml-ALT PNs had multiglomerular arborizations within the MGC, and were named Pml_a_MGC as they were similar to the Pml_a_OG neurons reported in Ian et al. (2016b) (Figure 8A; Appendix Figure 2B). Both Pml_a_MGC PNs passed off a side branch within the AL. In one preparation (#19) this side branch was seen exiting the AL ventral to the main axon and innervating areas in the LAL (see arrow in Figure 8A). In the other, (#20), the branch appears to innervate two adjacent glomeruli (not shown due to weak staining). Pml_a_MGC neurons projected laterally and terminated in the AVLP. Here, the main branch gave rise to numerous short side branches, each with several varicosities.

The third ml_ALT neuron, named Pml_c_OG, had a unique morphology by innervating only one single glomerulus, located in the postero-ventral region of the AL (Figure 8B). As other ml-ALT PNs, this neuron diverged from the m-ALT at the anterior edge of the central body, but continued dorso-laterally and bifurcated ventral to the pedunculus. One main branch projected ventro-laterally towards the lateral protocerebrum and diverged into several thinner fibers with numerous large swellings which terminated in the posterior lateral protocerebrum (PLP) (see arrow in Figure 8B) and partially in the LH. The main branch then projected postero-medially and terminated at the base of the calyces in the SLP. The other main branch continued posteriorly, parallel to the pendunculus, and terminated anteriorly to the calyces where it had many varicosities. The two bifurcated fibers thus appeared to have overlapping projection fields at the anterior base of the calyces in the SLP. From the point of bifurcation to their terminal areas in the LH and SLP, both main branches had several short, fine processes with several large swellings (see arrowheads in Figure 8B).

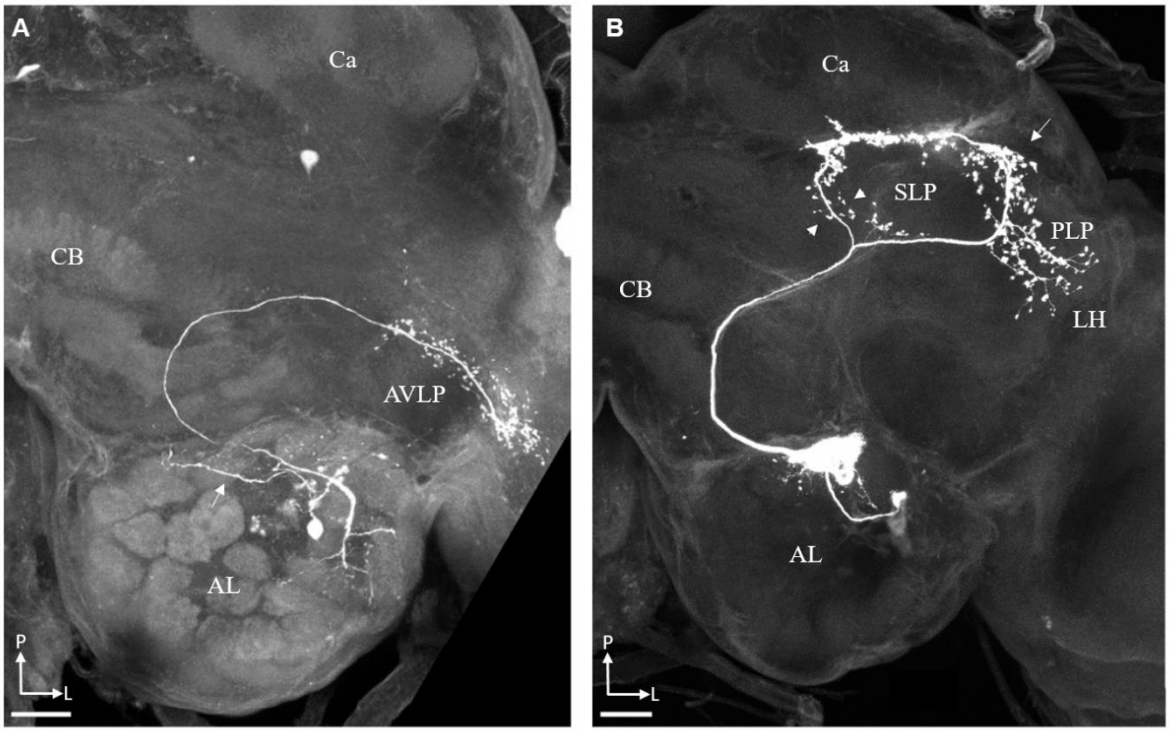

Figure 8. Confocal images of two projection neurons (PNs) in the medio-lateral antennal lobe tract (ml-ALT), in dorsal view. **(A)** A multiglomerular PN (#19) with soma in the lateral cell cluster (LCC), innervating all units of the MGC. A side branch can be seen bifurcating from the main axon within the antennal lobe (AL) (arrow). The axon bends laterally at the edge of the central body and projects directly to the anterior ventro-lateral protocerebrum (AVLP). **(B)** A uniglomerular ml-ALT PN (#21) with soma in the LCC. After turning laterally, the axon bifurcated and projected one branch to the posterior lateral protocerebrum (PLP) (indicated by the arrow) and the lateral horn (LH), and another branch to the base of the calyces (Ca), in the superior lateral protocerebrum (SLP). Note the small blebs extending from the two branches close to the bifurcation point (arrowheads). Scale bars: 50 µm.

3.1.3 l-ALT projection neurons

In this study, 4 l-ALT neurons were stained (two are shown as for examples, see Figure 9). Neurons in the l-ALT exited the AL ventral to the m-ALT and ml-ALT, and immediately projected laterally towards the lateral protocerebrum. They did not innervate the calyces. Three l-ALT PNs had the soma in the LCC, whereas soma location for the last preparation could not be determined due to weak staining.

One l-ALT PN, named the Pl_a_MGC PN, had dendritic ramifications within the cumulus and passed off side branches into the ishtmus after exiting the AL (see arrowhead in Figure 9A). The axon then continued laterally towards the lateral protocerebrum, where several short processes extended into the AVLP. The axon then turned about 90 degrees and continued dorso-medially, extending several short side branches and finally terminating anterior to the α-lobes, in the pillar-shaped structure known as the column (Ian et al., 2016a; Ian et al., 2016b).

One Pl_b_OG PN had dendritic arborizations in several ordinary glomeruli, and upon exiting the AL projected laterally toward the lateral protocerebrum (Figure 9B). A few side branches extended from the main axon into the ventromedial neuropil (VMNP) while the majority of branching occurred in the medial part of the AVLP. The axon finally terminated in two large club-like structures in the lateral part of the AVLP (see arrows in Figure 9B).

The two remaining l-ALT PNs could not be classified into subtypes due to insufficient staining of their terminal projections in the protocerebrum: one neuron had dendritic arborizations in multiple, ordinary glomeruli (see Appendix Figure 2C). The other weakly stained neuron projected through the l-ALT into AVLP (not shown).

3.1.4 t-ALT projection neuron

One t-ALT neuron was stained in one preparation (Figure 10). This neuron followed the same pathway from the AL as fibers in the m-ALT, but projected laterally at the posterior edge of the central body. The axon then bifurcated and innervated both the calyces and the lateral protocerebrum. As it was morphologically dissimilar to the t-ALT neuron reported in Ian et al. (2016b) it was classified as Pt_b type. The Pt_b neuron had soma in the LCC and dendritic innervations in several glomeruli, including OGs and the cumulus of the MGC. Dendritic innervations were particularly strong in one large glomerulus located ventrally in the AL (see dashed circle in Figure 10). Interestingly, two neurites originating from the main axon exited the AL ventrally and posterio-medially and projected ventrally (see arrows in Figure 10). However, due to weak staining, their terminal projection fields could not be

determined. Shortly after the axon diverged from the m-ALT pathway and bended laterally, it bifurcated and sent one branch posteriorly towards the calyces and another towards the lateral protocerebrum. The branch that innervated the calyces divided into several smaller fibers, each with numerous varicosities. The other branch projected to the PLP and the LH in the lateral protocerebrum. All branches contained numerous, small blebs. A single fiber with a small number of varicosities projected from the LH and back into the calyces (see arrowhead in Figure 10).

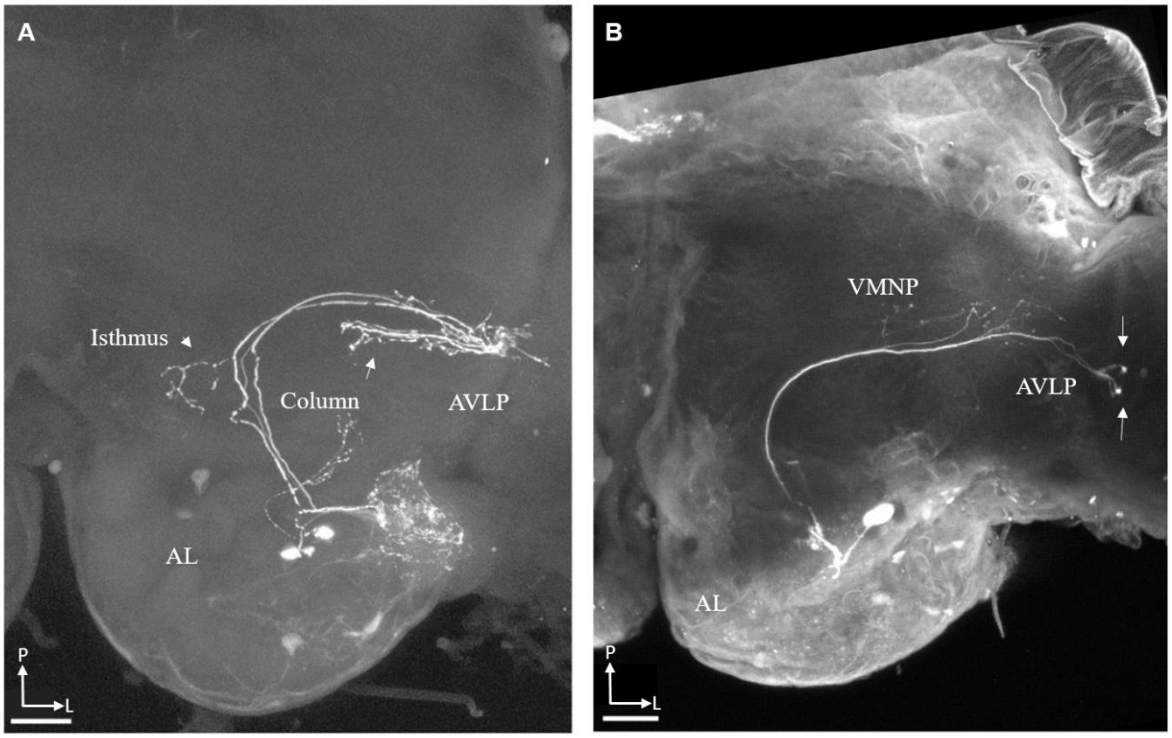

Figure 9. Confocal images of lateral antennal lobe tract (l-ALT) neurons, in dorsal view. **(A)** Three projection neurons (PNs) in the l-ALT (#24). All had cell body in the lateral cell cluster (LCC) and dendrites in the cumulus unit of the macroglomerular complex. A side branch extended into the isthmus (arrowhead). All projected to the anterior ventro-lateral protocerebrum (AVLP) and the column (arrow). **(B)** PN (#25) innervating ordinary glomeruli (not shown due to weak staining of dendrites), soma in the LCC. A few branches innervated the ventro-medial neuropil (VMNP), and the axon terminated in two club-like structures in the AVLP (arrows). Scale bars: 50 µm.

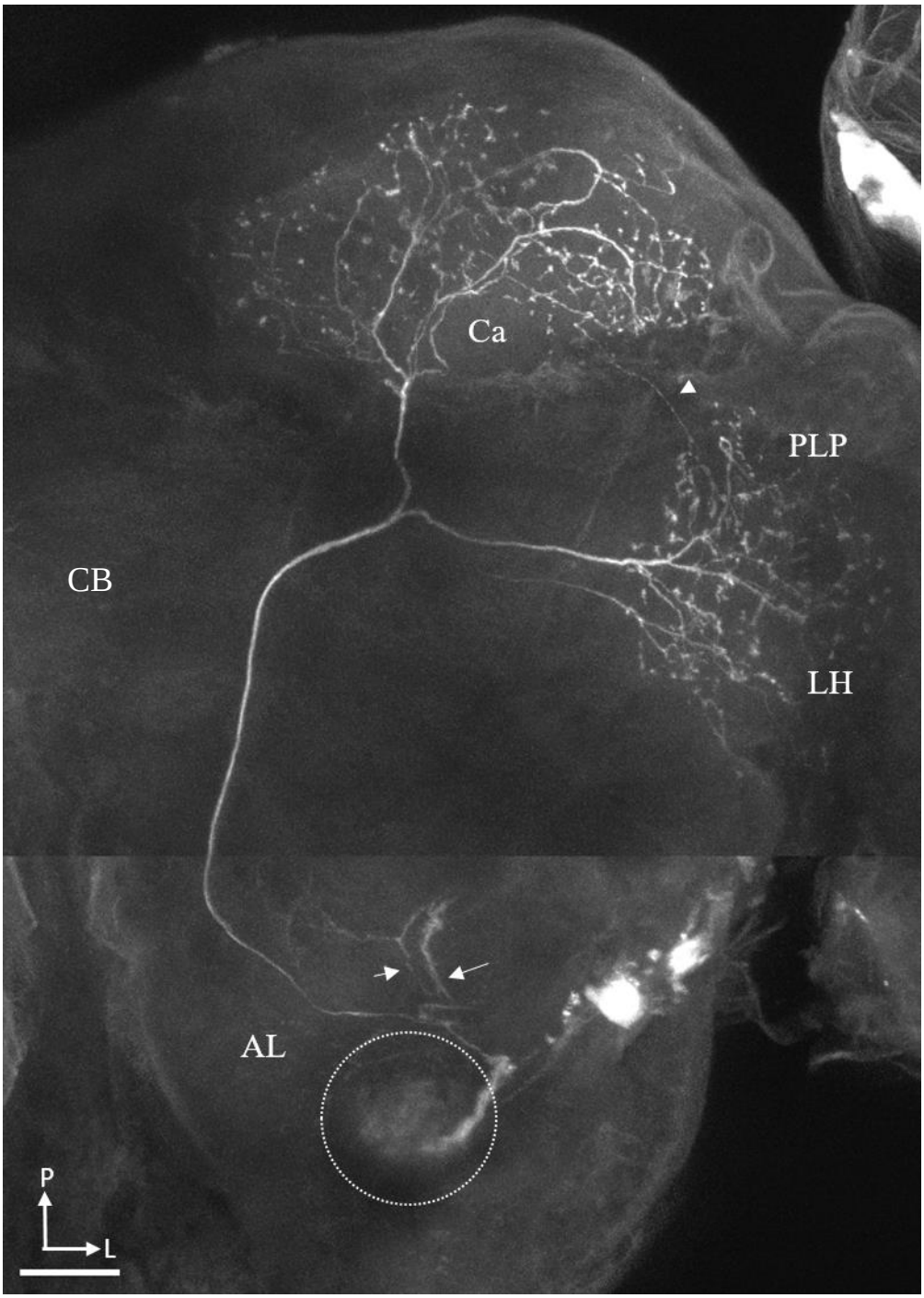

Figure 10. Confocal image of one projection neuron in the transverse antennal lobe tract (t-ALT) (#26), in dorsal view. The soma of this neuron was located in the lateral cell cluster. In the antennal lobe (AL) it had dendritic ramifications in all glomeruli (not shown due to weak staining). One glomerulus located ventrally in the AL was better stained than the remaining glomeruli (dashed circle). Two neurites extended ventrally towards the gnathal ganglion (arrows). However, due to insufficient staining they could not be traced completely. After turning laterally, the axon bifurcated and extended one branch into the calyces (Ca) and another into the lateral horn (LH) and the posterior lateral protocerebrum (PLP). A single neurite projected from the PLP to the calyces (arrowhead). CB, central body. Scale bar: 50 µm.

3.1.5 d-ALT projection neuron

Here, for the first time in heliothine moths, we describe the protocerebral projection fields of a d-ALT neuron that was stained in one preparation (Figure 11). This neuron (Pd type) projected dorso-laterally from the AL and innervated widespread regions of the lateral protocerebrum. It had dendritic arborizations in multiple glomeruli in one AL, and several side branches were seen extending from the main neurite (see arrow in Figure 11A, B, and arrowhead in Figure 11B). From the AL, the neurite bifurcated and sent one branch through the inferior antennal lobe commissure to the contralateral brain hemisphere, where its soma resided in the MCC The other branch projected postero-laterally towards the ventro- and dorso-lateral protocerebrum. Here, the main branch split into numerous blebby side branches that innervated the PLP, PVLP, AVLP, LH, and SLP. In the SLP, the branches went posterior and dorsal to the α-lobes. Additionally, a side branch diverged from the main neurite before it reached the LH and projected postero-dorsally into the calyces (see arrowhead in Figure 11A). Due to the co-staining of a multiglomerular LN, the exact dendritic ramifications of the Pd neuron in the AL could not be determined. However, given that several side branches parted from the main neurite within the AL, and that by Kanzaki et al. (1989) reported a multiglomerular Pd neuron, it is highly likely that the Pd neuron presented here also innervated several glomeruli.

3.2 Centrifugal neuron morphology

Two different types of CNs were recorded and stained in this study: the CSD neuron previously reported in several insect species (Dacks et al., 2006) and a previously unreported bilateral, paired centrifugal neuron.

3.2.1 Contralaterally projecting, serotonin-immunoreactive neuron

The CSD neuron, which was stained in two preparations (Figure 12), was morphologically similar to the CSD neurons reported in *M. sexta* (Kent et al., 1987), *P. americana* (Salecker & Distler, 1990), *B. mori* (Hill et al., 2002), and *H. assulta* (Zhao & Berg, 2009). In all these insect species, the CSD neuron had a large soma in one AL, dendritic ramifications in large areas of the superior, lateral protocerebrum in both hemispheres, and terminal output synapses in all glomeruli in the contralateral AL. However, as compared to the previous report from the heliothine moth, *H. assulta*, the CSD neurons presented here

were substantially better stained (particularly one preparation, i.e. Figure 12A). Therefore, the morphology of this widespread neuron is considerably more accurately described here.

The primary neurite from the soma projected posteriorly along the m-ALT pathway. In the postero-dorsal protocerebrum, the neurite bifurcated and extended one thick branch laterally where it innervated regions in the ipsilateral SLP, LH, and the calyces. The other branch crossed the midline through the superior postero-lateral protocerebral commissure, and projected to the contralateral hemisphere. Here, it bifurcated into several side branches, which innervated large areas of the SLP and LH, but not the calyces. The dendritic ramifications in the SLP were extensive and had a meshwork-like appearance. The innervation pattern in the two hemisphere was asymmetrical, and in the contralateral SLP. Additionally, the main branch in the contralateral hemisphere passed off one neurite that continued along the m-ALT pathway into the AL, and another neurite that extended towards the central body (see arrows in figure 12B). The former neurite entered the contralateral AL (relative to the soma) where it densely innervated every glomeruli. The latter neurite passed off numerous short side branches as it projected antero-medially towards the midline (see arrow in Figure 13A). Dorsal to the central body, the neurite bifurcated and extended a single process into the central body (see arrowhead in Figure 13A). Here, it innervated the entire posterior region of the central body. From the point of bifurcation, the remaining neurite continued postero-dorsally and appeared to join the large branch in the ipsilateral (relative to the soma) protocerebrum.

Interestingly, one CSD neuron (#30) extended a single branch anteriorly towards the LAL and innervated areas around the α-lobes, although its precise location could not be determined due to deformation of the brain (see dashed circle in Figure 13A). This CSD neuron also had branches in the ipsilateral SLP that contained varicose, blebby terminals, indicative of presynaptic boutons (see dashed circle in Figure 13B). Furthermore, the same preparation Although the CSDs neuron mainly had uniform glomerular innervation pattern throughout the AL (Figure 13c), one preparation (#28) had particularly strong innervation of a single glomerulus located ventro-medially in the AL (see dashed circle in Figure 13D).

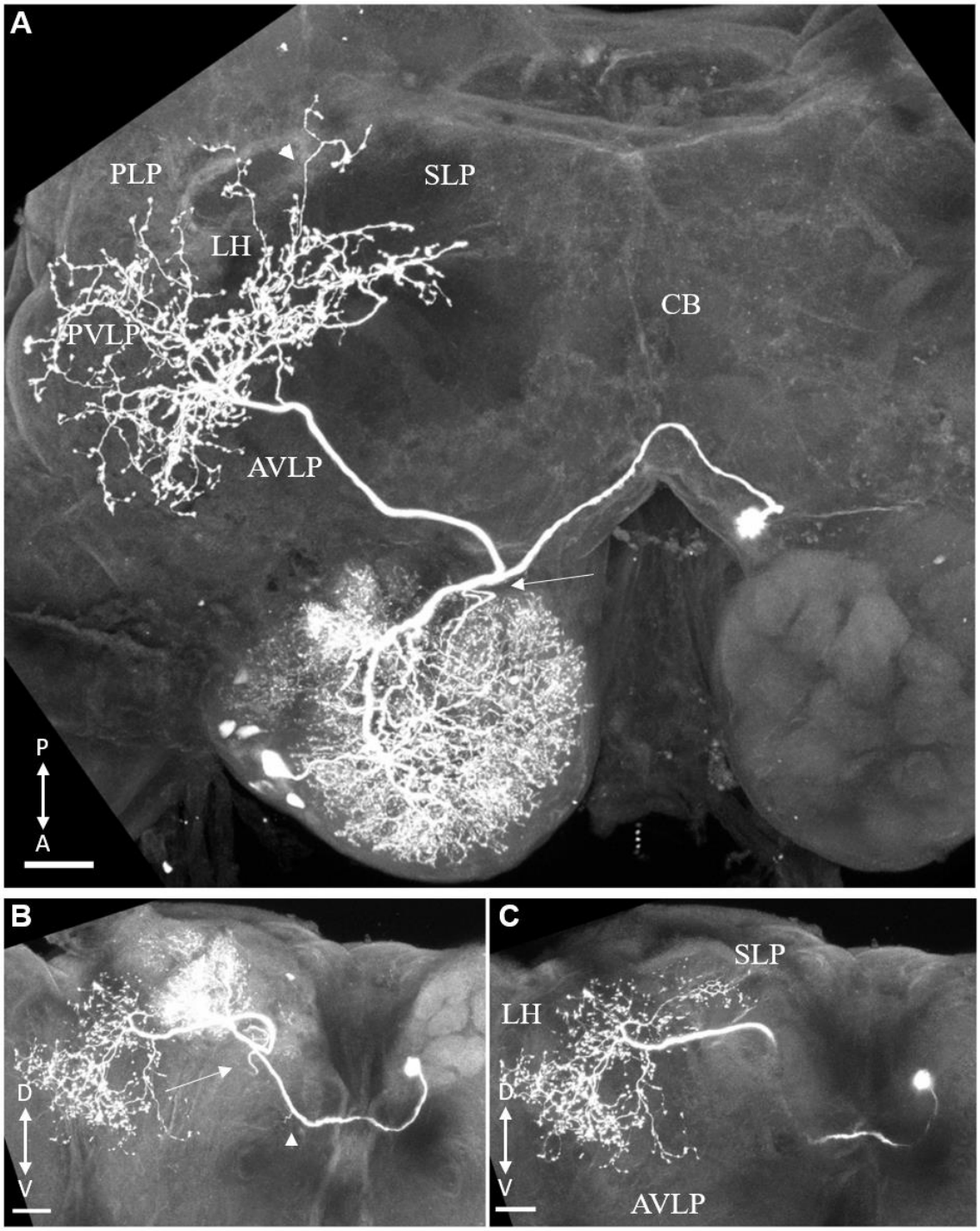

Figure 11. Confocal images of one neuron in the dorsal antennal lobe tract (d-ALT) (#27). **(A)** Dorsal view. This projection neuron (PN) had multiglomerular arborizations in the antennal lobe (AL) and soma in the medial cell cluster in the contralateral AL. It had widespread innervation of several regions in the lateral protocerebrum: anterior ventro-lateral protocerebrum (AVLP), lateral horn (LH), posterior lateral protocerebrum (PLP), posterior ventro-lateral protocerebrum (PVLP), and superior lateral protocerebrum (SLP). A single branch also extended into the calyces (Ca) (arrowhead). As the axon entered the AL, two neurites bifurcated and innervated multiple glomeruli (arrow) **(B)** Frontal view. Same neurites extending from the axon (arrow). An additional branch projected from the axon into the AL (arrowhead). **(C)** Frontal view. The projection fields of this neuron extended ventrally, in the AVLP, and dorsally, in the SLP. CB, central body. Note that a local interneuron (LN) with soma in the lateral cell cluster was co-stained in this preparation. Scale bars: 50 µm.

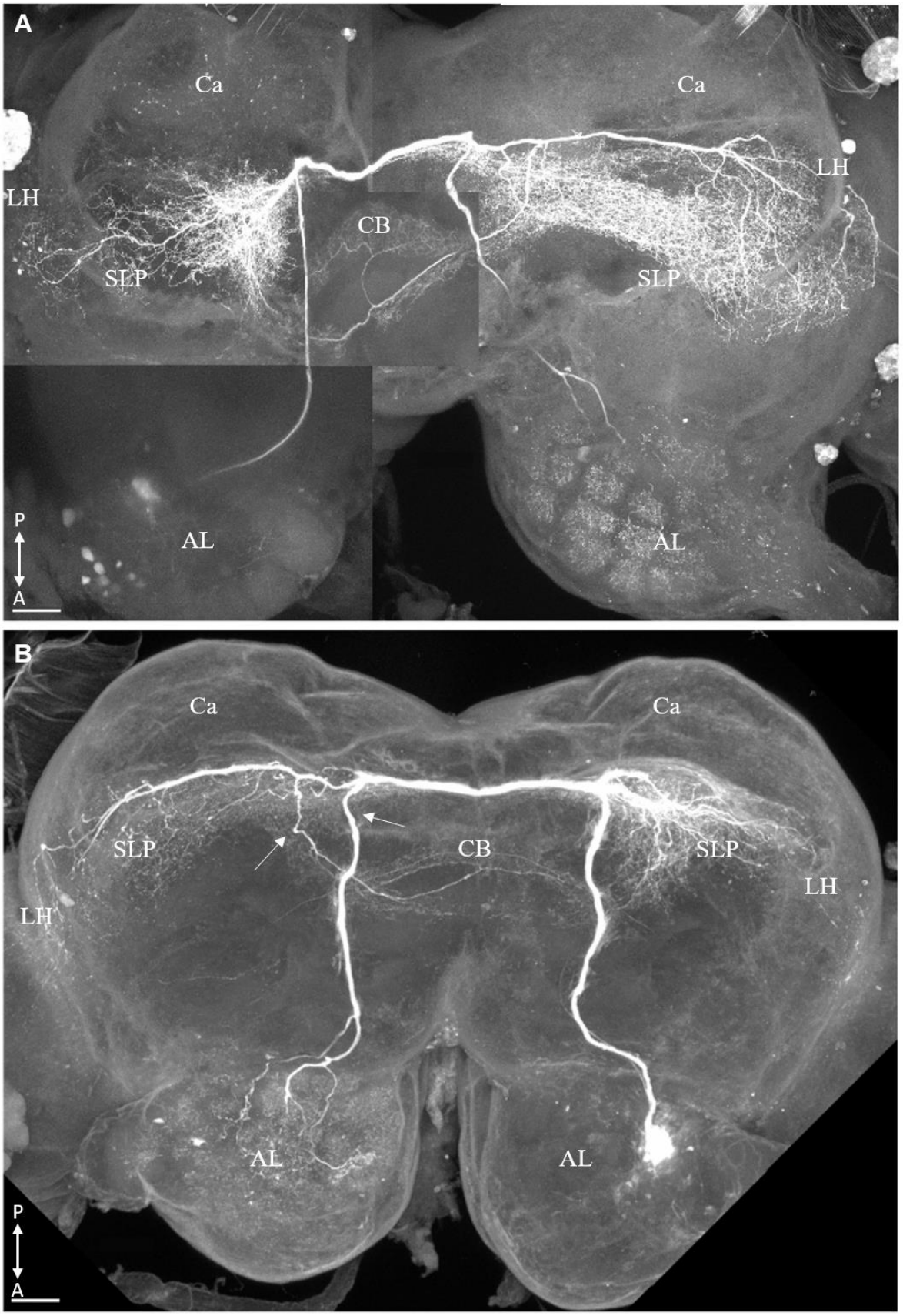

Figure 12. Confocal images of two contralaterally projecting, serotonin-immunoreactive deutocerebral (CSD) neurons (#30-31), in dorsal view. **(A-B)** The soma of the CSD neuron resided in the postero-ventral region of one antennal lobe (AL). From the soma, the primary neurite projected via the m-ALT

into the posterior protocerebrum where it bifurcated. One branch continued laterally into the ipsilateral superior lateral protocerebrum (SLP), lateral horn (LH), and calyces (Ca). The other branch crossed the midline via the postero-lateral protocerebral commissure, and extended into the contralateral SLP and LH. Two neurites extended from the contralateral branch (arrows, **B**). One followed the m-ALT and innervated all glomeruli in the contralateral AL. The other branch projected antero-medially and innervated the central body (CB). Scale bars: 50 µm.

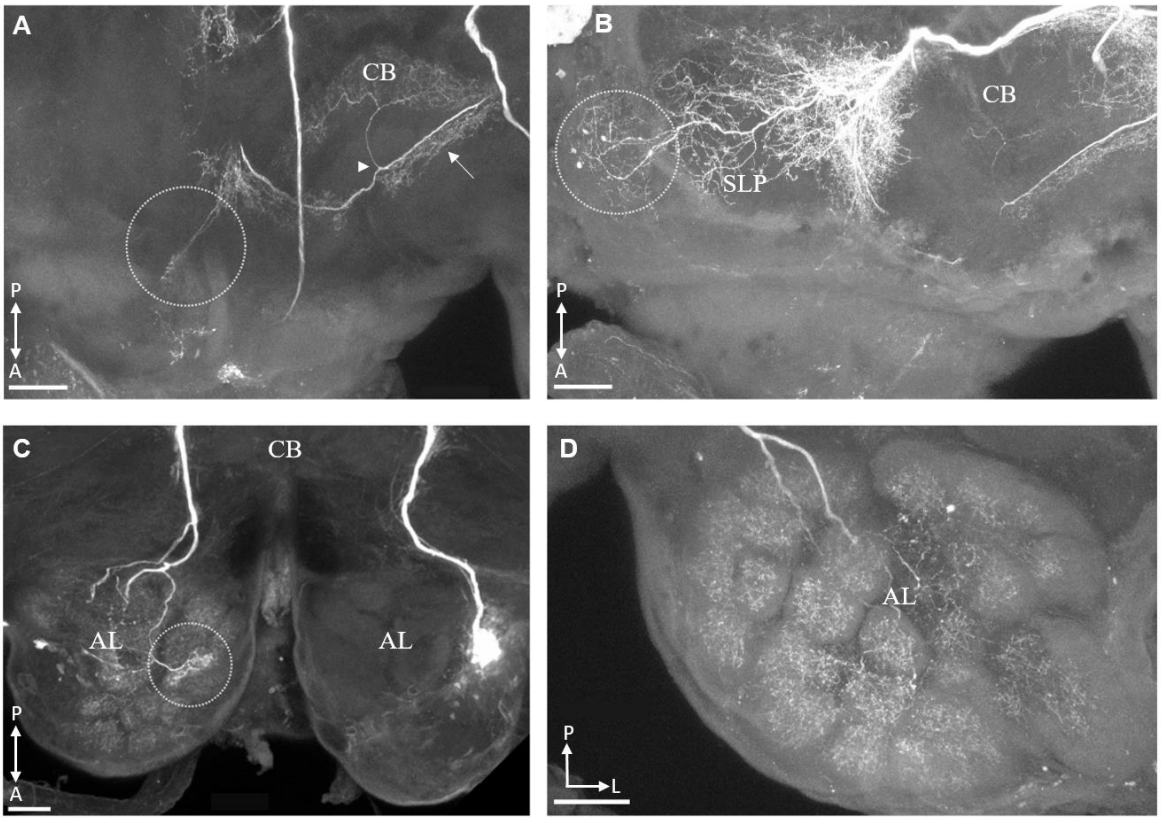

Figure 13. Confocal images of the contralaterally projecting, serotonin-immunoreactive deutocerebral (CSD) neuron, in dorsal view. **(A)** One CSD neuron (#30) had a branch that projected towards the lateral accessory lobe. As the brain was slightly deformed, the precise innervation of this branch could not be determined. One neurite extended from the protocerebral branch and projected towards the central body (CB) (arrow). Dorsal to the CB, it bifurcated and innervated the posterior region of the CB. **(B)** Same CSD neuron also had varicose blebs, indicating presynaptic terminals, in some processes in the ipsilateral (relative to the soma) branch in the superior lateral protocerebrum (SLP). **(C)** One CSD neuron (#31) exhibited particularly strong innervation of a single glomerulus (dashed circle). **(D)**. Uniform, innervation of all glomeruli in the antennal lobe (AL). Scale bars: 50 µm.

3.2.2 Bilateral paired centrifugal neuron

Here we report a type of bilateral, paired centrifugal (BPC) neuron not previously described in any insect species (Figure 14). The cell body of this neuron was located in the protocerebrum, it had widespread dendritic ramifications in the dorsomedial regions of both brain hemispheres and synaptic terminal output seemingly inn all glomeruli in both ALs. The

neurites which projected to the AL resided outside of all known ALTs. Recording and staining from this neuron type was obtained from two different preparations. In these two preparations, the soma was located in opposite hemispheres, indicating that each neuron mirrors the other and that there is at least one pair of morphologically 'identical' neurons.

Both stained neurons had a soma (~20 µm in diameter) located in a cell cluster positioned ventral to where the pedunculus exits the calyces. The primary neurite extending from the soma projected anteriorly and dorso-medially towards the midline of the brain. Dorsal to the central body, just prior to reaching the midline, the neurite bifurcated. One neurite extended anteriorly, while the other neurite continued over the midline to the contralateral hemisphere. Then, the neurites in both hemispheres of the brain each contacted a large-diameter branch that projected laterally. Both of these thick branches bifurcated into several smaller processes, which innervated large regions of the SLP and superior intermediate protocerebrum (SIP). Smooth neurites, absent of varicosities and blebs, generally indicates dendritic processes (Cardona et al., 2010). Two thin neurites extended from one hemisphere to the other (see arrows in Figure 14A). From the dorsomedial protocerebrum, both large-diameter branches then projected medially and antero-ventrally into the ALs. Here, each branch formed sparse innervations in almost every glomeruli (see Figure 15).

Interestingly, this neuron did not innervate any of the lobes, despite extensive dendritic ramifications in the protocerebrum (see Figure 15). Some dendritic processes were seen innervating the anterior optic tubercle (see arrow in Figure 15A) and others targeted areas that surrounded the Y tract, an additional fiber bundle projecting from the calyces observed in heliothine moths (Rø et al., 2007), (see arrows in Figure 15B). The neurites that projected to the ALs entered ventro-medially, medial to the β-lobes (see arrows in Figure 15C). No staining was observed in one glomerulus in the contralateral AL (relative to the soma), located medially to the dm-a and dm-p unit of the MGC (see dashed circle in Figure 15D). 1-2 thin branches containing a low number of blebs innervated the remaining glomeruli in both ALs. These terminal projections had fewer branches with larger varicosities as compared to the CSD neurons (Figure 13D).

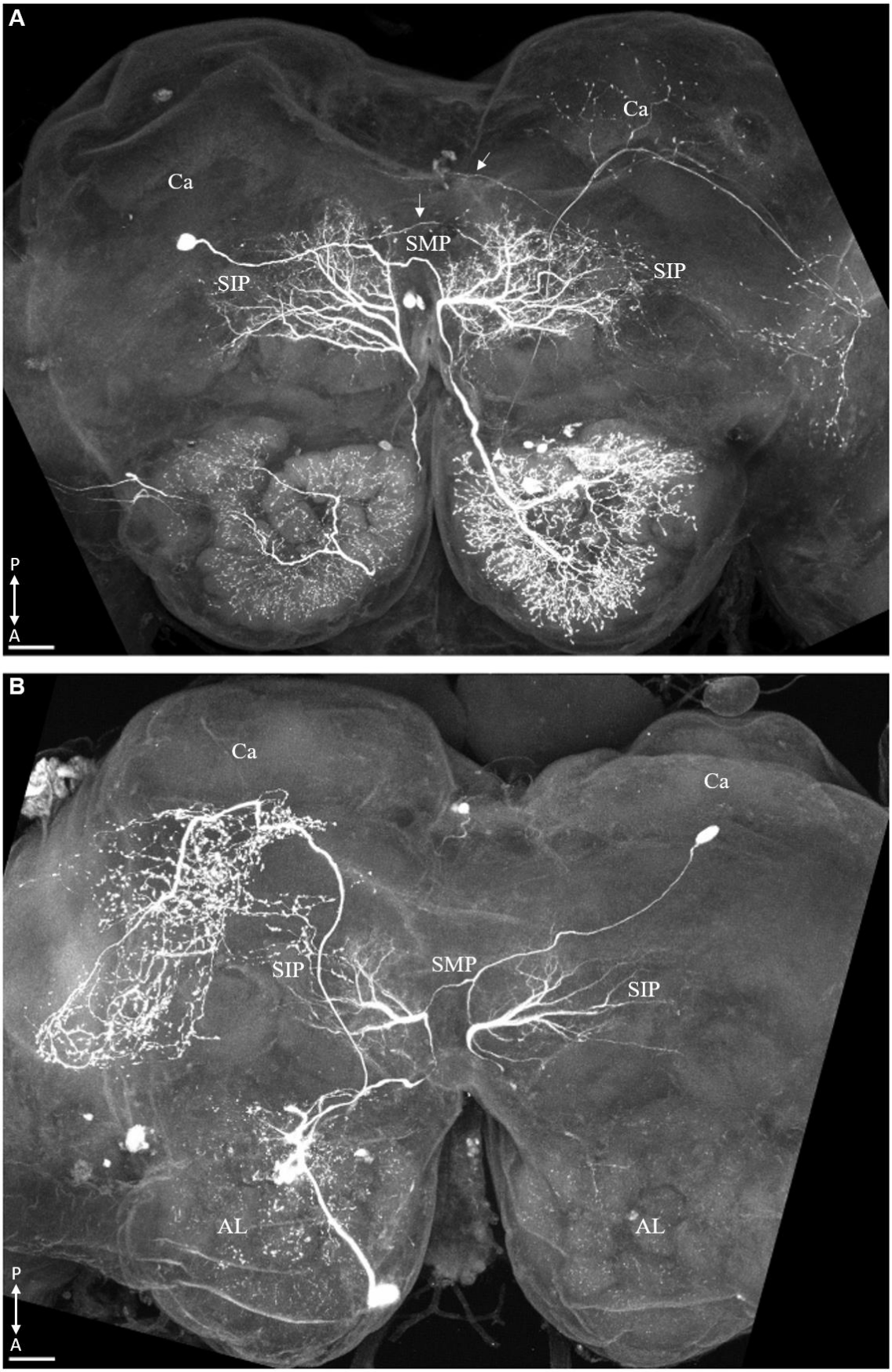

Figure 14. Confocal images of two bilateral, paired centrifugal (BPC) neurons (#28-29), in dorsal view. **(A-B)**. The soma of the BPC neuron was located ventral to where the pendunculus exits the

calyces (Ca). From the soma, the primary neurite projected anteriorly and dorso-medially. Close to the midline, the neurite bifurcated and extended one neurite anteriorly, while the other crossed the midline. In the superior medial protocerebrum (SLP), both neurites contacted a large-diameter branch which projected laterally into the SLP and superior intermediate protocerebrum (SIP). Here, the thick branch bifurcated into several side smooth processes, indicating dendritic processes. From each of the two thick branches, a thinner branch continued antero-ventrally and entered the antennal lobes (ALs) ventrally. In the AL, each branch bifurcated and sparsely innervated almost all glomeruli. Note that in **(A, B)**, another neuron was co-stained with the BPC neuron. In (A), 2-3 projection neurons in the m-ALT innervated the calyces and the lateral horn (LH). A descending neuron is also stained in the left AL. In (B), the additional neuron had soma in the anterior cell cluster, projected in the m-ALT and innervated large regions of the lateral protocerebrum. Scale bars: 50 µm.

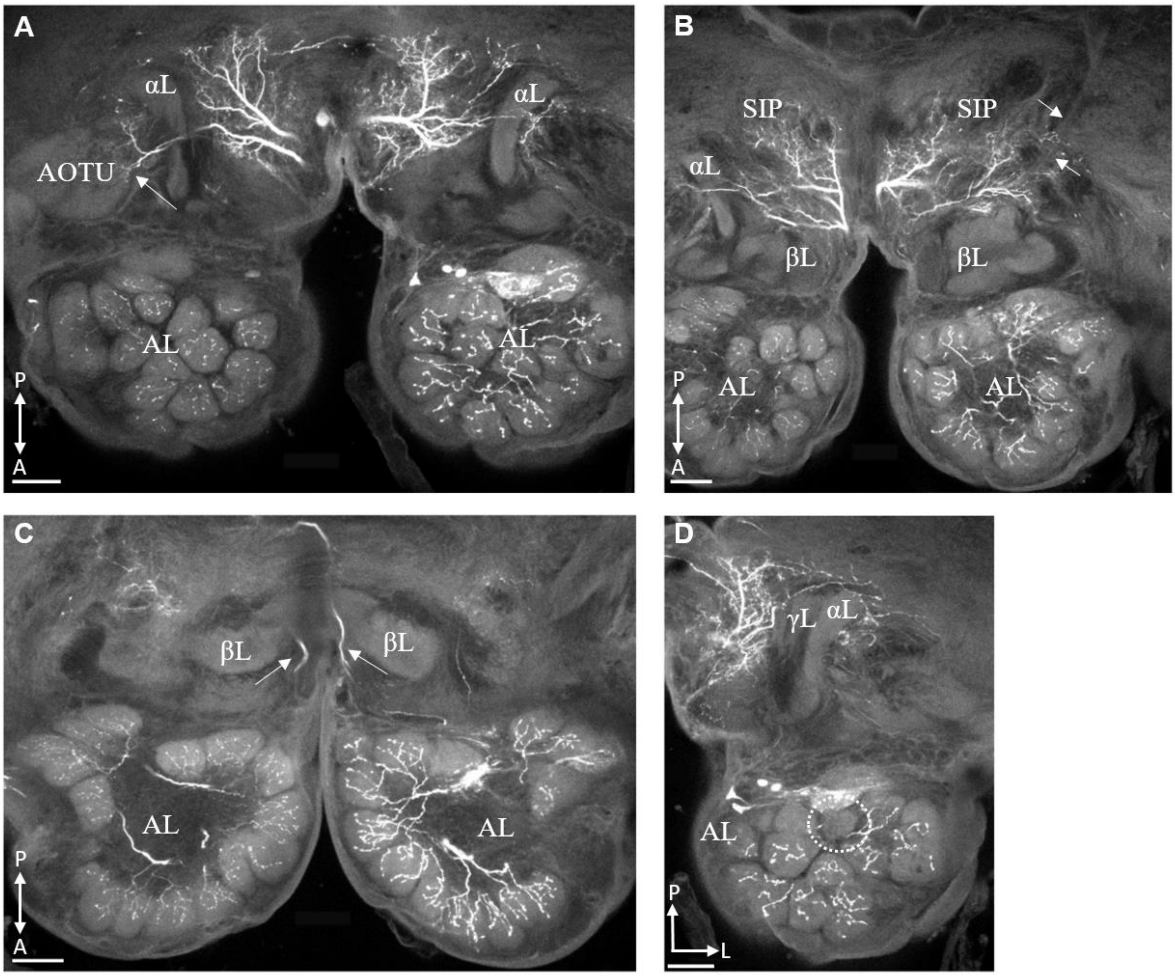

Figure 15. Confocal images of the bilateral, paired centrifugal (BPC) neuron, in dorsal view. Note the sparse innervation of almost every glomeruli and the absence of innervation in any of the mushroom body lobes. **(A)** A single branch was observed extending into the anterior optic tubercle (AOTU) (arrow). **(B)** The BPC neuron innervated regions surrounding the Y tract (arrows) and the superior intermediate protocerebrum (SIP), but not any of the lobes. **(C)** From each large branch in superior medial protocerebrum and SIP, two neurites projected antero-ventrally (arrows). These did not enter the antennal lobes (ALs) through any of the antennal lobe tracts. Rather, they entered medially and ventrally. **(D)** The BPC neuron had sparse innervation in all glomeruli, except for a single glomerulus located medially to the macroglomerular complex (dashed circle). βL, beta-lobe; αL, alpha- lobe; γL, gamma-lobe. Scale bars: 50 µm.

3.3 Physiological responses of projection neurons and centrifugal neurons to odorant stimuli

An overview of the level of activation (number of spikes) in PNs and CNs during the presence of odorant and control stimuli is displayed in figure 17. Regarding the most numerous PN category, the m-ALT PNs, the majority of neurons did not exhibit differences in the firing rate did not change during odor or control stimulation from the pre-stimulus firing rate. A subset of m-ALT PNs (#1-5) exhibited increased firing rate in response to multiple odorants, whereas some m-ALT PNs (#4, 7-8, 16-18) decreased their firing rate in response to one or several odorants. Of the three ml-ALT PNs reported here, the two with glomerular ramifications within the all units of the MGC (#19-20) showed an increase in firing rate to one or several stimuli, particularly to the pheromone blend and primary pheromone component, but not to the control. As the ml-ALT PNs, all l-ALT PNs (#22-25) demonstrated increasing firing rate in response to one or several stimuli. One l-ALT PN (#24) identified as innervating the MGC, had particularly strong increase in firing rate in response to the pheromone blend. In another l-ALT PN (#22), both the pheromone blend, secondary component, and interspecific antagonist elicited high levels of spiking activity.

In the CNs, presentations of various odorant stimuli elicited only modest increases in firing rate, as compared to baseline. However, an exception was seen in one CN (#29). This neuron exhibited a modest increase in firing frequency to the pheromone blend, Z11-16:AL, and sunflower extract (see Appendix Figure 4). Although the firing rate was not as high as the responses obtained in some PNs, they were still distinguishable from the pre-stimulus spontaneous activity which was very low. Neither CSD neurons responded to pheromone or plant odors or control stimulus.

Figure 16 shows the classification of CN and PN responses, based on a comparison to the number of spikes elicited by odor stimuli and the control stimulus (see method section: Quantification and visualization of physiological responses). The majority of m-ALT PNs were classified as not responding to the odorant stimuli. Of the m-ALT PNs that were classified as having excitatory and inhibitory responses, all but one (#17) responded only to a single stimulus (either excitatory or inhibitory). Irrespective of ALTs, the pheromone blend elicited excitation in four MGC PNs (#8, 19-20, 24), whereas one MGC PN (#9) was inhibited by the sunflower extract. Three OG PNs (#5, 7, and 16) were inhibited by the sunflower extract. One m-ALT PN (#17) and one l-ALT PN (#22) had a mixed response profile, demonstrating excitation to one stimulus and inhibition to others. The ml-ALT MGC PNs had excitatory responses to more than one stimulus, a pattern that also was seen in one l-

ALT PN (with mixed response profile) and one CN. Despite the increase in firing rate observed in PNs belonging to various ALTs to several stimuli (see above), this change was often not significant when compared to level of activity evoked by the control stimulus. For instance, both ml-ALT PNs exhibited increased firing rate to several odorants. However, when analyzed quantitatively and compared to response during presentation of control stimulus, only the primary pheromone component (Z11-16:AL) and the pheromone blend elicited significant responses.

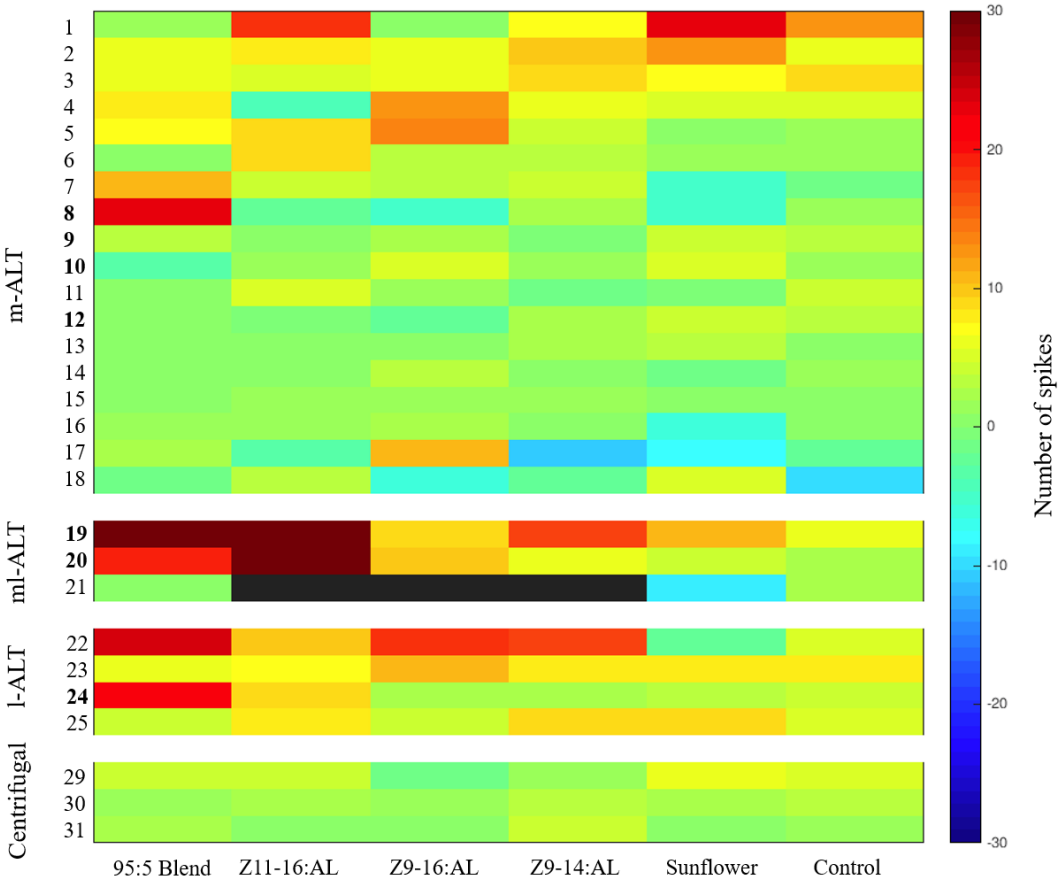

Figure 16. Color-plot of the range of responses (based on the number of significant spikes; see Method section 2.5.2 Quantification and visualization of physiological responses) of individual neurons (PN *n* = 25; CN *n* = 3) to a 95:5 blend of the primary (Z11-16:AL) and secondary (Z9-16:AL) pheromone component, the primary (Z11-16:AL) component, the secondary (Z9-16:AL) component, the interspecific antagonist (Z9-14:AL), sunflower extracts, and control (hexane). Neurons within each category (m-ALT, ml-ALT, l-ALT, and centrifugal) were ranked in ascending order of mean response intensity.

To further compare PN and CN responses to the odor stimuli, the response classifications (excitatory, inhibitory, no response) of morphologically identified MGC (*n* = 7) and OG PNs (*n* = 13) were compared to the response classifications of CNs (*n* = 3) (Figure 17). Plant odors generally do not activate MGC PNs, and vice versa for pheromones and OG PNs. Therefore, MGC PNs were compared with CNs in their response to the pheromone blend (Figure 17A), while OG PNs were compared with CNs in their response to the sunflower extract (Figure 17B). Four MGC PNs (#8, 19-20, 24) had excitatory responses to the pheromone blend, and interestingly, so did one CN neuron (#29). This neuron also responded with excitation to the sunflower extract. In comparison, the sunflower extract elicited excitation in one OG PN (#18) and inhibition in four OG PNs (#5, 7, 16, 21).

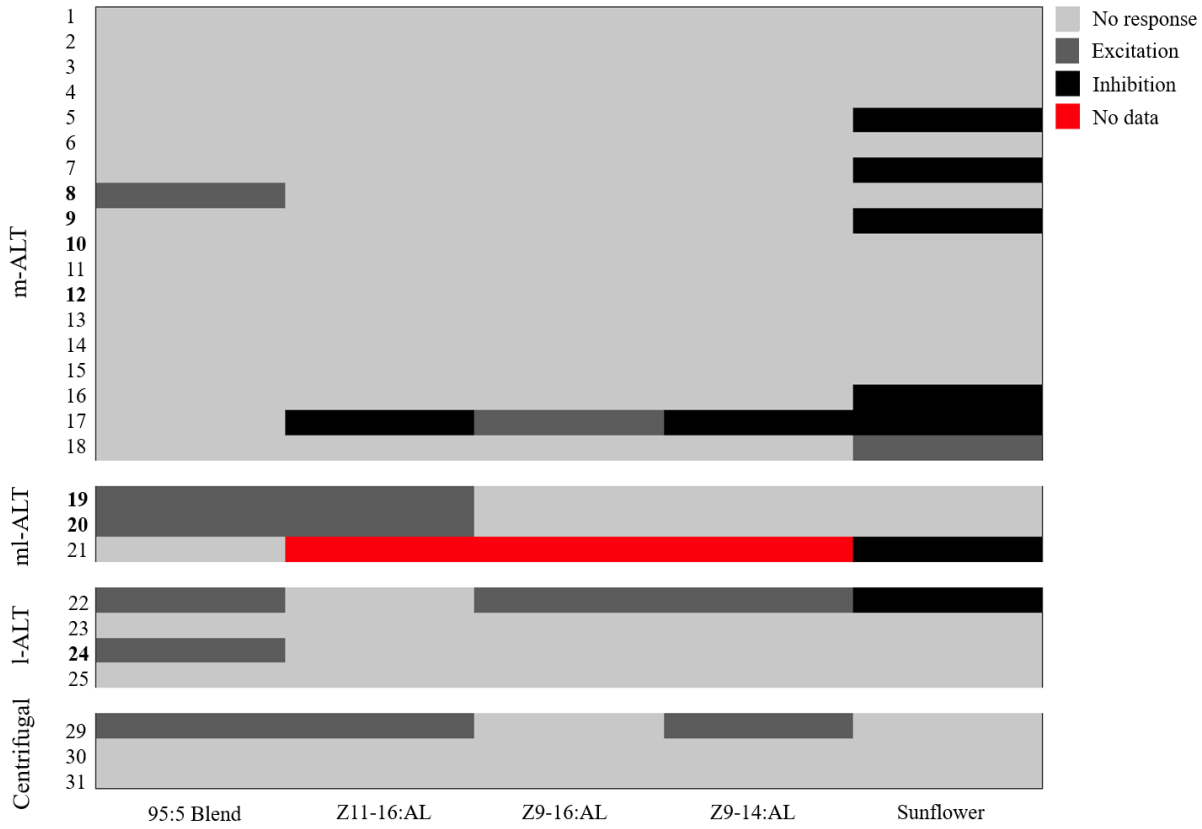

Figure 17. Response plot showing the classification of the responses of individual neurons (PN *n* = 25; CN *n* = 3) to a 95:5 blend of the primary (Z11-16:AL) and secondary (Z9-16:AL) pheromone component, the primary (Z11-16:AL) component, the secondary (Z9-16:AL) component, the interspecific antagonist (Z9-14:AL), sunflower extracts, and control (hexane). Each response was classified as either excitatory, inhibitory, or no response. Red bars indicates that stimuli was not tested. Neurons are follow the same rank as in Figure 16.

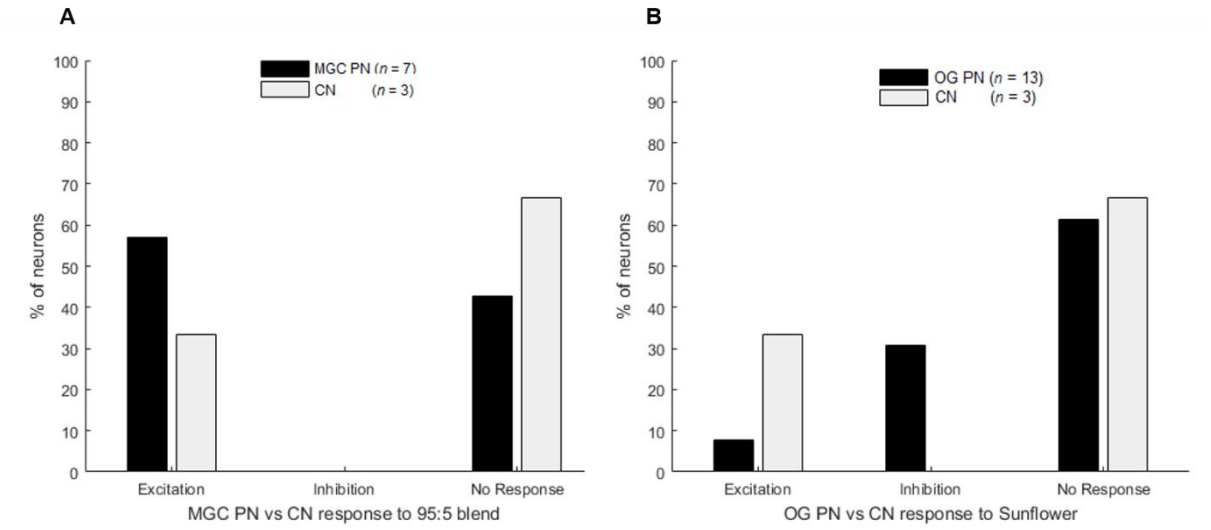

Figure 18. Histograms of the percentage of neurons that exhibited excitation, inhibition, or no response. **(A)** The responses of projection neurons innervating the macroglomerular complex to 95:5 blend of the primary (Z11-16:AL) and secondary (Z9-16:AL) are compared against the responses of centrifugal neurons. **(B)** The responses of projection neurons innervating ordinary glomeruli to the sunflower extract are compared against the responses of centrifugal neurons.

Stimulation with pheromone- and plant odors elicited different excitatory response patterns which were categorized based on the temporal length of the responses, spiking frequency, as well as the co-occurrence of inhibition (Figure 19). The various excitation patterns were independent which ALT the PNs projected in or whether the PNs innervated OG or the MGC. Additionally, neurons would occasionally exhibit different excitation pattern to different stimuli. Thus, individual PNs were not classified according physiological response. Three types of physiological responses were seen in this study: monophasic, biphasic, and triphasic response patterns.

A common monophasic response to pheromone or plant odors consisted of an increase in firing rate shortly after the stimulus is introduced, which continues during the entire length of the stimulus window (400ms) and for a short time after, before it resumed spontaneous firing activity (short tonic response, Figure 19A). A less frequent monophasic response pattern comprised of long-lasting excitatory (LLE) tonic response (Figure 19B). Here, the firing rate increased first at the end of the stimulus presentation and then continued for several seconds after the end of the stimulus presentation. Other neurons exhibited biphasic and triphasic response patterns characterized by initial excitation subsequently followed by inhibition (Figure 19C-E). One biphasic response pattern was characterized by a tonic

excitation in which firing rate was increased for the remainder of the stimulus duration followed by inhibition of spiking activity (Figure 19C). In comparison, the other biphasic response pattern exhibited a short excitatory burst of spikes, which were subsequently inhibited for the remainder of, and a short time period after, stimulus presentation (Figure 19D). The triphasic response pattern (phasic-tonic-inhibition) observed in some neurons consisted of an initial short burst of spikes, then increased levels of firing rate during stimulus presentation and then inhibition of spiking activity (Figure 19E). In contrast to the heterogeneous nature of the excitatory responses, the all inhibitory responses constituted a single, monophasic inhibitory response pattern (Figure 19F). Generally, the spiking activity ceased shortly after presenting the stimulus and the inhibition continued for the remainder of the stimulus duration and for a short period after, and then resumed pre-stimulus spontaneous activity firing rate.

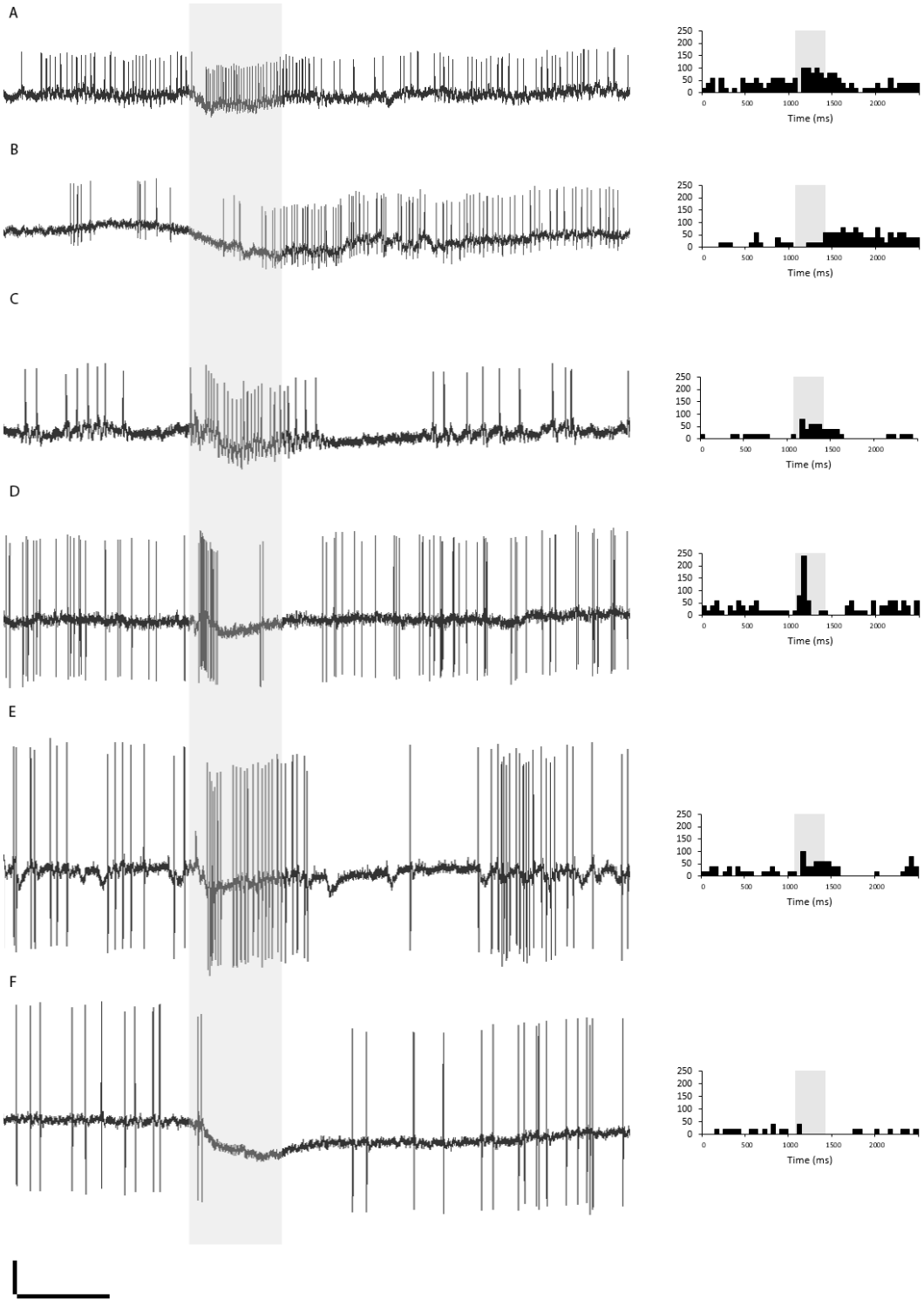

Figure 19. The examples of response patterns of projection neurons, raw data on the left, PSTH displaying spikes/second on the right. Duration of stimulus presentation indicated by the transparent grey bar **(A)** Monophasic excitatory response, consisting of tonic firing lasting approximately the length of the stimulus. **(B)** Monophasic, long-lasting excitation (LLE). Firing rate is tonic and prolonged, even after stimulus offset. **(C)** Biphasic response, consisting of tonic firing lasting the length of the stimulus, followed by inhibition. **(D)** Biphasic response, consisting of a rapid, phasic burst followed by inhibition. **(D)** Triphasic response: A rapid, phasic burst of spikes is followed by tonic firing for the remainder of the stimulus duration, and finally inhibited. **(F)** Monophasic inhibition. Generally, all inhibitory responses were similar: inhibition began shortly after stimulus onset and briefly outlasted the duration of the stimulus. Scale bars: 10mV, 400ms.

4. Discussion

Here, we have used intracellular recording and iontophoretic staining in combination with confocal microscopy to elucidate the morphological and physiological characteristics of projection neurons and centrifugal neurons. The 25 identified PNs were confined to one of five different ALT: the medial, medio-lateral, lateral, transverse, and dorsal tract. (Actually, the only tract missing is the dorso-medial ALT). The results presented here broadens the previous anatomical descriptions of PNs in moths (Homberg et al., 1988; Ian et al., 2016b; Rø et al., 2007) by describing the complete morphology of a uniglomerular ml-ALT PN and a t-ALT PN subtype, neither of which are reported previously. Furthermore, we present the first anatomical examination of a d-ALT PN in heliothine moths.

Four CNs constituting two distinct categories were identified. One of these categories includes a previously unreported centrifugal neuron with widespread dendritic and terminal projections in the insect brain. The other category implies the CSD neuron. Here, we expand on the original morphological description of CSD neurons in heliothine moths provided by Zhao and Berg (2009).

Regarding physiological response properties, we obtained responses to pheromone and plant odors in some of the PNs: MGC PNs responded primarily to pheromones, whereas OG PNs responded to plant odors (e.g., Christensen & Hildebrand, 1987; Christensen et al., 1991; Christensen et al., 1995). One CN responded to both pheromone and plant odors, suggesting a role for this neuron in the olfactory processing of both pheromone and non-pheromone odors.

4.1 Structural and functional organization of the parallel olfactory pathways

4.1.1 Projection neurons are narrowly or broadly tuned to odors

The majority of PNs reported in the present study belonged to one of the three classical ALTs (i.e., the m-ALT, ml-ALT and l-ALT). Of these, most PNs were confined to the m-ALT and all morphologically identified m-ALT PNs were categorized as the Pm_a subtype. These results are consistent with earlier findings showing that the m-ALT is the most prominent in terms of number of PNs, and consists mainly of homogeneous PNs with uniglomerular dendritic arborizations and terminal projection fields in the calyces and LH (Anton & Homberg, 1999; Homberg et al., 1988; Ian et al., 2016b; Rø et al., 2007). Generally, uniglomerular PNs are narrowly tuned and respond preferentially to one key odorant during low stimulus concentration (King et al., 2000; Reisenman et al., 2004; Reisenman et al., 2005). In support of this, we show that of the majority of uniglomerular PNs in the m-ALT

exhibit little or no response to most of the tested stimuli, including the primary (Z11-16:AL) and secondary (Z9-16:AL) pheromone components, a pheromone blend, interspecific signals (Z9-14:AL), and sunflower extracts containing plant volatiles which activates multiple types of OSNs in heliothine moths (Røstelien et al., 2005). Of those m-ALT neurons that did respond to odor stimulation, each neuron typically only responded to a single odor. Similarly, the novel, uniglomerular neuron projecting in the ml-ALT (#21) exhibited highly specific responses only to one odor (sunflower extract). This selective response to specific odors among neurons arborizing within a single glomerulus suggest that odor tuning is determined by innervation pattern in the AL. Taken together, this indicates that uniglomerular PNs signal the presence of a particular odor in the environment, and may encode the identity of an odor.

Conversely, most neurons in the ml-ALT and l-ALT presented in the current study, and those reported previously in other insect species (e.g., Abel, Rybak, & Menzel, 2001; Homberg et al., 1988; Ian et al., 2016b; Løfaldli, Kvello, Kirkerud, & Mustaparta, 2012; Rø et al., 2007; Tanaka et al., 2012a), had dendritic arborizations within all or most glomeruli and projected mainly to the lateral protocerebrum. In this study, we demonstrated that most ml-ALT and l-ALT PNs exhibited increased firing rates to several or all odor stimuli (**Figure 12, 13**). Broader response profiles in multiglomerular PNs, as compared to uniglomerular PNs, have also been seen in *D. Melanogaster* (Wang et al., 2014). It is likely that ml-ALT and l-ALT PNs exhibit a broader odor tuning than uniglomerular neurons due to their multiglomerular arborizations pattern within the AL. This type of dendritic innervation pattern offers the possibility of integrating information across several glomeruli. Consequently, multiglomerular neurons should be less able to discriminate among odors, as sufficient activation of any innervated glomerulus would elicit a response in that neuron. Thus, neurons arborizing in multiple glomeruli may signal the general presence of an odor stimulus, but do not discriminate among odors.

A small subset of OG m-ALT PNs did, however, also exhibit a modest excitatory response to several stimuli including control. Low frequency excitation during presentation of a clean air puff or hexane has been observed in previous reports of OG and MGC PNs (Christensen et al., 1991; Han et al., 2005; Jarriault et al., 2009; Kanzaki et al., 1989), and it has been proposed that PNs may receive mechanosensory input in addition to olfactory input. In support of this, Han et al. (2005) observed that mechanosensory neurons in the noctuid moth *Spodoptera littoralis* had terminal projections within the antennal mechanosensory and motor center and the AL. The same study also found that a number of PNs that were excited by mechanosensory input exhibited increased levels of activity when mechanosensory input

was presented together with pheromones. The authors suggested that integration of odor and wind stimuli in the AL enhances orientation in an odor plume during up-wind flight.

4.1.2 Comparison of the pheromone and non-pheromone pathways

Projection neurons that innervated the male-specific MGC, exhibited anatomical and functional characteristics which were distinctly different from neurons innervating ordinary glomeruli, in accordance with previous reports (e.g., Christensen & Hildebrand, 1987; Homberg et al., 1988; Kanzaki et al., 2003; Seki et al., 2005; Zhao & Berg, 2010). Notably, the dendrites of MGC PNs were restricted to one or multiple units of the MGC, and their axons mainly projected to regions of the lateral protocerebrum (AVLP, SLP, column), and, more sparsely, in the calyces of the MB. In comparison, non-pheromone PNs innervated OG and terminated mainly in the calyces of the MB and LH. In agreement with the anatomical findings, MGC PNs and OG PNs were also functionally distinct: neurons innervating OG and MGC showed virtually no overlap in their physiological responses, and were preferentially tuned to plant volatiles and pheromones, respectively.

Two neurons which innervated the cumulus unit of the MGC, one m-ALT PN (#8) and one l-ALT PN (#24), responded highly specific to the pheromone blend, thus exhibited the characteristics of a "blend-specialist" (e.g., Anton & Hansson, 1995; Hartlieb et al., 1997; Lei & Hansson, 1999; Wu et al., 1996). The two MGC neurons projecting in the ml-ALT (#19-20) showed high level of activation to multiple odors. However, they responded particularly strong to the pheromone blend and to the primary pheromone component (Z11-16:AL). The two PNs confined to the medio-lateral tract may therefore be classified as "component-specific" neurons. It has been proposed that the selective preference for the pheromone blend, here seen in two "blend-specialist" and two "component-specific" neurons, may determine the simultaneous arrival of individual pheromone components in a blend (Vickers, 2006). Additionally, Christensen and Hildebrand (1997) observed that some MGC PNs respond more strongly to the pheromone blend than to the individual pheromone components (synergism); the blend also allows the MGC PNs to accurately track a pulsed pheromone presentation aimed to mimic a naturally occurring pheromone plume. This increased sensitivity for the pheromone blend likely reflects that many MGC PNs are maximally tuned to detect the naturally occurring ratio of the primary and secondary pheromone component released by the conspecific female.

In comparison, OG PNs responded only to the sunflower extract and not to any of the pheromone components or the blend. Of the morphologically identified OG PNs, four (#5, 7,

16, 21) were inhibited by the sunflower extract, while one (#18) exhibited an excitatory response. Interestingly, the innervated glomeruli of three of four OG PNs that where inhibited by the sunflower extract were located in the same dorso-lateral region of the AL (see dashed circles in Appendix Figure 3).

A few neurons did show some overlap in their responses to pheromones and plant odors. Notably, one MGC PN in the m-ALT (#9) was inhibited by the sunflower extract. In a previous study, some PNs were shown to exhibit excitatory responses to both pheromones and plant volatiles (Anton & Hansson, 1995). Some overlap in the physiological responses of MGC and OG PNs might be expected as LNs suppress firing activity in some glomeruli to enhance the signaling of other glomeruli (lateral inhibition). According to this, one may observe inhibition in MGC PNs during stimulation with plant volatiles, and vice versa in OG PNs when stimulating with pheromones. The inhibitory response during the presence of plant odors, seen in one m-ALT MGC neuron here, appears to give some support to this idea.

Generally, however, the results presented here confirm the existence of compartmentalized subsystems in the olfactory system of insects, which is structurally and functionally specialized to detect and process pheromone and plant information, respectively. Pheromone-sensitive PNs arborize exclusively in the MGC and respond preferentially to pheromones. In the lateral protocerebrum, these neurons target an area that is spatially separated from the output regions of PNs innervating non-pheromone glomeruli. The differences in innervation pattern between MGC PNs and OG PNs in the calyces of the MB further suggests that pheromone and non-pheromone odors play different roles in learned, odor-evoked behaviors. As MGC PNs have sparse innervation of the calyces, pheromone information appears to be more directly conveyed to regions of the lateral protocerebrum that mediates innate, experience-independent behaviors. Contrary, odor information conveyed by OG PNs may be involved in behaviors dependent on previous experience and environmental cues. Unlike pheromones, which are rare and offer a very specific signal detected by a sensitive olfactory sub-system, plant odors come in vast numbers in the environment, only some of which are relevant to the organism (i.e. offering possibilities of food or oviposition). In such an ambiguous environment, the ability to associate contextual cues, such as biologically non-relevant plant odors or visual features of the landscape, with biologically relevant plant odors, may offer an adaptive advantage for the organism.

4.1.3 The response patterns of projection neurons

In the current study we have shown that there is considerable heterogeneity of odor-evoked excitatory response patterns among PNs in the different ALTs. This is in correspondence with previous studies of PN physiology (Barrozo et al., 2011; Christensen & Hildebrand, 1987; Christensen et al., 1991; Christensen et al., 1995; Jarriault et al., 2009; Kuebler et al., 2011; Løfaldli et al., 2012; Zhao & Berg, 2010).

The monophasic response pattern consisting of long-lasting excitation (LLE) was observed in two OG PNs in response to sunflower extract and one MGC PN in response to pheromone blend. Similar results have been reported both for MGC PNs (Lei & Hansson, 1999) and OG PNs (Løfaldli et al., 2012), and in some protocerebral neurons in response to pheromones (Iwano et al., 2010; Kanzaki et al., 1991; Lei et al., 2001). These findings raise an important question: is the LLE observed in AL and protocerebral neurons mediated by the same underlying mechanism? Other studies have hypothesized that the LLE in protocerebral olfactory neurons originates within the MB or LAL (Iwano et al., 2010; Kanzaki et al., 1991). However, the results presented here raises the possibility that LLE at the central level (protocerebral olfactory neurons) originates in the AL, based on intrinsic connections of OSNs, LNs, and PNs (a similar hypothesis was proposed by Lei & Hansson, 1999). If this is the case, then LLE in PNs may be relayed to higher olfactory centers, including the LAL. Interestingly, LLE in the LAL is assumed to underlie the zigzag searching locomotion in male upwind flight in response to pheromones (Iwano et al., 2010). Thus, LLE originating in the AL may directly contribute to this behavioral response. The monophasic, short excitatory responses were less frequently observed among PNs in the current study, although others have reported an equal distribution of excitatory, inhibitory, and biphasic responses (Kuebler et al., 2011). Based on an increase in spiking activity when a stimulus was presented in high concentrations as compared to low concentrations, Kuebler et al. (2011) hypothesized that this response pattern encodes stimulus concentration. In both monophasic responses, the absence of inhibition following the initial excitation imply that PNs exhibiting these responses are not influenced by GABAergic LNs.

Two out of five response profiles exhibited a biphasic, mixed response pattern in which an initial excitation was followed by inhibition. This response pattern is frequently observed in PNs (Barrozo et al., 2011; Jarriault et al., 2009; Lei & Hansson, 1999). Lei and Hansson (1999) discuss that this PN response pattern could arise from by initial excitation from OSNs, and subsequent inhibition from LNs, which are also postsynaptic to OSNs. Alternatively, OSNs excite PNs, which in turn form presynaptic connections to LNs. The LNs

would then be activated and inhibit the PNs. However, the differences observed between the response patterns (i.e. tonic-inhibition, phasic-inhibition) suggests that precise interactions between OSNs, LNs, and PNs differ. Specifically, unlike the phasic-inhibition pattern, the tonic-inhibition response pattern exhibits continued firing throughout the stimulus duration followed by inhibition of spiking activity. Thus, LN inhibition appears to occur first at the offset of the stimulus. This feature may allow PNs to encode the duration of the stimulus, whereas it has been proposed that the phasic-inhibition response pattern would allow PNs to accurately encode pulsed pheromone signals in an odor plume (Christensen & Hildebrand, 1997; Lei & Hansson, 1999).

The triphasic, mixed response pattern, phasic-tonic-inhibition, is less common but has occasionally been observed in PNs (Jarriault et al., 2009). Similar to the biphasic tonic-inhibition pattern, it appears that the late inhibition would also allow PNs with this response profile to encode the duration of the stimulus. However, the addition of an initial phasic phase may serve to rapidly signal the presence of a stimulus.

In contrast to the excitatory response patterns, the inhibitory responses observed in this study were homogeneous and closely matched stimulus duration, similar to what previous studies have found (Christensen & Hildebrand, 1987; Jarriault et al., 2009; Kuebler et al., 2011). Differences in inhibitory responses have been observed, but then as an ability to follow pulsed stimulus signals (Lei & Hansson, 1999). It is possible that similar findings could have been observed in the current study if stimuli had been presented as a series of short pulses instead of one single pulse.

4.2 Centrifugal neurons have widespread arborizations in the protocerebrum and output terminals in the antennal lobe

4.2.1 Morphological and physiological properties of the contralaterally projecting, serotonin-immunoreactive deutocerebral neuron

The morphological features of the CSD neurons presented in the current study correspond to those seen in previous reports of this neuron in other insect species (Coates et al., 2017; Dacks et al., 2006; Hill et al., 2002; Kent et al., 1987; Zhao & Berg, 2009). Notably, the soma of the CSD neuron resided in the postero-ventral region of one AL, it had asymmetrical dendritic ramifications covering vast regions of both protocerebral hemispheres, and terminal output areas in all glomeruli in the contralateral AL. The particularly strong staining of one CSD neuron (#30) allowed us to expand on the previous anatomical

description of this neuron. Importantly, we were able to demonstrate an extensive meshwork of branches in the lateral protocerebrum, suggesting that this area provides considerable input to this neuron. Furthermore, we demonstrate that the CSD neuron also extends branches into the central body and the calyces, similar to observations in *M. sexta* (Kent et al., 1987). The current findings thus elaborates on the previous observation of the CSD neuron in the heliothine moth, *H. assulta* (Zhao & Berg, 2009), in which no innervations of the central body or calyces were seen. Given the strong staining obtained from one neuron in the current study, the lack of innervation of these areas reported by Zhao and Berg (2009) likely stems from insufficient staining of the neuron, rather than actual morphological differences.

In other insect species, such as the moth *B. mori* and the fruit fly, *D. melanogaster*, the CSD neurons pass off neurites that innervates the ipsilateral LAL shortly after exiting the AL (Dacks et al., 2006; Hill et al., 2002). The LAL is a pre-motor center which mediates signals between the central body and thoracic motor centers, and serotonin-like immunoreactivity has been observed in fibers in the LAL (Namiki & Kanzaki, 2016). Thus, it is possible that the CSD neurons mediates serotonergic modulation of both olfactory processing in the AL and of motor pathways in these species. However, no innervation of the LAL was observed here, nor in previous reports from *H. assulta* (Zhao & Berg, 2009) and *M. sexta* (Kent et al., 1987). It therefore appears that the CSD neuron possess morphological characteristics that differs across species, and consequently, that it may serve somewhat different functions depending on the insect species.

Previous examinations of the physiological responses of the CSD neuron have yielded ambiguous results. In the moth *B. mori*, pheromone and control stimuli (hexane) stimuli both evoked an excitatory response, thus indicating a mechanosensory response (Hill et al., 2002). Zhao and Berg (2009) reported a CSD neuron that exhibited excitation to several pheromone components, the blend and the plant oil ylang-ylang. These findings were interpreted as an olfactory response, although a mechanosensory response were not ruled out due to lack of control stimulus testing. Interestingly, this CSD neuron also contained two sets of spikes, which differed in amplitude, duration, and firing rate (responses were seen only in the smaller set of spikes). This finding might be a result of the recording site. They recorded from the AL containing the synaptic output/dendritic terminals, and it is possible that these neurites possess multiple zones in which spikes can be initiated. In contrast to these findings, a recent study in *D. melanogaster* observed inhibitory responses to a wide range of plant and pheromone odors, except for ammonia which elicited an excitatory response (Zhang & Gaudry, 2016). In the present study, we demonstrate that neither plant volatiles nor pheromones elicits any response

in the CSD neuron in *H. armigera*. The absence of response to the clean air puff demonstrate that it is not sensitive to mechanosensory stimuli. Despite the fact that studies have demonstrated that the CSD neuron receive presynaptic connections from certain, glomerulus-specific OSNs in the AL (Coates et al., 2017; Sun et al., 1993), it is likely that it receives the majority of input from the extensive dendritic ramifications in the superior and lateral protocerebrum of both hemispheres, rather than from the AL. Thus, the evidence put forward here suggests that rather than providing feedback to the AL based on olfactory processing, the CSD neuron modulates AL processing based on input from non-olfactory networks, possibly related to other sensory modalities or the general state of the animal.

4.2.2 Morphological and physiological properties of the bilateral, paired centrifugal neuron

The morphological features of the BPC neuron presented in the current study are characteristic of modulatory centrifugal neurons: The cell body is located outside of the AL in the protocerebrum; they have extensive, varicose branches that indicates presynaptic terminals, which projects to all or most glomeruli; and fine, dendritic ramifications in large parts of the protocerebrum. To the best of our knowledge, this neuron have not been reported in previous studies of the insect brain. Mass staining of the AL in *M. sexta* (Homberg et al., 1988) and *H. virescens* (Ian et al., 2016a; Zhao et al., 2013a) have failed to show this neuron. One explanation of this result may be that CNs on a general basis are not shown in mass staining of the AL due to the low number of such neurons in the brain resulting in less absorption of dye than PNs. Mass staining of the AL did, however, reveal the CSD neuron (Kent et al., 1987). As the BPC neurons only have sparse glomerular innervation in the AL, it is possible that they are less likely to absorb dye. Additionally, neither immunostaining with GABA (moths: Berg et al., 2009; Hoskins et al., 1986; fruit fly: Okada, Awasaki, & Ito, 2009), octopamine (fruit fly: Busch, Selcho, Ito, & Tanimoto, 2009), histamine (reviewed by Nässel, 1999), nor serotonin (moth: Kent et al., 1987) have revealed this neuron. However, the presence of a large number of neuroactive substances the AL (reviewed by Homberg & Müller, 1999) as well as electrically coupled synapses in the AL (Yaksi & Wilson, 2010), suggests many alternative, possible mechanisms for this neuron to interact with other AL neurons.

The cell body of the two BPC neurons are located in opposite hemispheres in the two preparations, which indicates that each neuron is mirrored by a morphologically 'identical' neuron, similar to the previously described CSD neurons. Unlike the CSD neurons, which have asymmetrically projections in the brain, the functional need for paired, symmetrical

centrifugal neurons is less apparent. One explanation is that the neurons differ slightly in micro-level morphology in the ALs. For instance, the CSD neuron receive glomerulus-specific input in the AL (Coates et al., 2017; Sun et al., 1993). It is possible that each BPC neuron also possess an innervation pattern in the AL that is variant between these neurons. Further studies are needed to determine how the BCP are wired to intrinsic AL neurons, and if they also receive input and provide output in the AL.

The BPC neurons have bilateral and largely symmetrical dendritic ramifications in the SMP and SIP. These areas partially overlap with another CN, the multisensory ARM/VIR neurons reported by Zhao et al. (2013a). However, these neurons also innervated the inferior neuropils (INP) located more ventrally. Unfortunately, only olfactory stimuli were tested here, making it impossible to say whether the BPC neuron also respond sensory stimuli in other modalities. The SMP and SIP are unstructured neuropils and little is known of their function. However, mass staining of the SMP in *B. mori* have shown that it is connected to a several regions, including AVLP, SLP, MB, LAL, and CB (Namiki, Iwabuchi, Pansopha Kono, & Kanzaki, 2014). In the same study, single cells innervating both the SMP and LAL were excited by stimulation with pheromones, which suggests that the SMP participates in the pheromone-processing circuit. Little is known about the third-order olfactory neurons projecting from the LH in moths. However, based on the responding pattern of the BPC neuron, it is possible that also plant odor information is relayed to SMP. The physiological data obtained from the BPC neuron indicates that this neuron participates in the processing of both pheromones and plant odors. Specifically, we observed excitatory responses to the pheromone blend, the primary pheromone component (Z11-16:AL), and sunflower extract. Based on the bilateral projections in the protocerebrum and the ALs, we may speculate that this neuron receive both pheromone and plant odor information from the two hemispheres and provide feedback to intrinsic AL neurons. Further physiological studies of the BPC neuron should aid our understanding of its functional role in the insect brain.

4.3 The functional role of projection neurons and centrifugal neurons

Projection neurons are the principal output neurons from the primary olfactory center in the insect brain, the antennal lobe (Wilson & Mainen, 2006). Here, we have demonstrated PNs in five of the six parallel tracts (m-ALT, ml-ALT, l-ALT, t-ALT, d-ALT, and dm-ALT) that have been reported in moths (Homberg et al., 1988; Ian et al., 2016a; Ian et al., 2016b). These neurons innervated a single or multiple glomeruli and projected through one of the ALTs to higher brain regions, including the calyces of the MB and lateral protocerebrum,

regions that are involved in learned and innate odor-evoked behaviors, respectively. Through the physiological responses obtained from PNs in the current study, we show that odor signals that are detected by peripheral OSNs and conveyed to the AL, are transferred to higher brain regions by the PNs. Centrifugal neurons, on the other hand, generally have extensive, widespread dendritic ramifications throughout the protocerebrum and provide modulatory input to all or most glomeruli in both ALs. Our physiological data indicates that some CNs (e.g., BPC) may provide direct feedback to intrinsic AL neurons, based on olfactory processing in the AL which in turn activates the CNs. Others may modulate the AL activity, and alter sensory threshold and behavioral responses based on the internal state of the animal (Lizbinski & Dacks, 2018) or input from non-olfactory sensory modalities, e.g. sound (Zhao et al., 2013a).

4.4 Methodological considerations

The main aim of the current study was to examine the morphological and physiological characteristics of PNs and CNs involved in olfactory processing. Some considerations of the current study are worth mentioning. The variation of odorants tested for each neuron was rather small, which makes the subsequent analysis of each neurons odor tuning somewhat restricted. However, a wider range of odorants indicates a longer time would be needed to test all stimulations. As a stable contact with a neuron only could be kept for 5-15 minutes while using the sharp-electrode technique, inclusion of additional odorants would likely have reduced the success rate of data collecting. Therefore, to keep a relevant high success rate of experiments and at the same time test as many odorants is thus a tradeoff any researcher must consider. Yet, the design of the stimulations used in this study included multiple pheromone components and a sunflower mixture consisting of several components known to activate OSNs, were sufficient to gain new insights in PN and CN physiology. Furthermore, the sample largely consists of neurons in the m-ALT, which is a result of both the number of neurons in this ALT but also the sampling strategy. Notably, the microelectrodes were inserted postero-medially in the AL where the thick axons left the AL. This positioning increased number of successful individual staining of neurons (as compared to when sampling from other parts of the AL), but at the cost of acquiring more m-ALT neurons.

The inclusion of quantitative analyses of neuronal responses in addition to visual inspection was made to add statistical rigor to the analyses and to transition from the subjectivity and bias inherent in human observers and to more objective calculation of

responses to odorants. In doing so, we are aware that such an approach has limitations, and that there exists no perfect algorithm able to determine what is and is not a neuronal response. Rather, this should be seen as the first steps in an approach which may eventually result in objective, standardized calculation of neuronal responses to stimuli.

The quality of the stained neurons using the fluorescent dye differed substantially among various preparations. This difference depended largely on the contact between the recording electrode and the neuron. Preparations frequently contained dye leakages and/or multiple stained neurons. Whenever the morphology of various neuron types was described, descriptions were made of the best stained preparation(s).

5. Conclusions

- The staining of 25 PNs confined to one of five parallel ALTs points out the significance of parallel olfactory processing in the moth brain. The generally good quality of the stained preparations made it easy to classify all AL output neurons according to the tracts.

- The majority of stained PNs consisting of uniglomerular medial-tract neurons responding more specifically than multiglomerular PNs in other tracts indicates the prominent role of the m-ALT in odor identification.

- The finding of multiglomerular PNs in the lateral and medio-lateral ALT, which responded more broadly to odors, indicates that these paths serve functions different from odor identification.

- Among the stained neurons was one notable PN confined to the dorsal ALT, described for the first time in heliothine moths.

- Another newly described type of PN, was a uniglomerular output neuron passing along the ml-ALT. Most previously described PNs confined to this tract were multiglomerular.

- A new centrifugal neuron, named BPC, previously not described in any insect species, was discovered in the present study. The odor-evoked responses in the BPC neuron suggests that it functions as feedback neuron.

- The high-quality staining of the serotonin-immunoreactive centrifugal neuron obtained in this study, allowed detailed description of this neuron's morphology in the heliothine moth.

References

Abel, R., Rybak, J., & Menzel, R. (2001). Structure and response patterns of olfactory interneurons in the honeybee, *Apis mellifera*. *Journal of Comparative Neurology, 437*(3), 363-383. doi:doi:10.1002/cne.1289

Ache, B. W., & Young, J. M. (2005). Olfaction: Diverse Species, Conserved Principles. *Neuron, 48*(3), 417-430. doi:https://doi.org/10.1016/j.neuron.2005.10.022

Anton, S., & Hansson, B. S. (1995). Sex pheromone and plant-associated odour processing in antennal lobe interneurons of male *Spodoptera littoralis* (Lepidoptera: Noctuidae). *Journal of Comparative Physiology A, 176*(6), 773-789. doi:10.1007/bf00192625

Anton, S., & Homberg, U. (1999). Antennal Lobe Structure. In B. S. Hansson (Ed.), *Insect Olfaction* (pp. 17-124). Germany: Springer.

Barrozo, R. B., Jarriault, D., Deisig, N., Gemeno, C., Monsempes, C., Lucas, P., Gadenne, C., & Anton, S. (2011). Mating-induced differential coding of plant odour and sex pheromone in a male moth. *European Journal of Neuroscience, 33*(10), 1841-1850. doi:doi:10.1111/j.1460-9568.2011.07678.x

Berg, B. G., Schachtner, J., & Homberg, U. (2009). γ-Aminobutyric acid immunostaining in the antennal lobe of the moth *Heliothis virescens* and its colocalization with neuropeptides. *Cell and Tissue Research, 335*(3), 593-605. doi:10.1007/s00441-008-0744-z

Berg, B. G., Zhao, X. C., & Wang, G. (2014). Processing of Pheromone Information in Related Species of Heliothine Moths. *Insects, 5*(4), 742.

Busch, S., Selcho, M., Ito, K., & Tanimoto, H. (2009). A map of octopaminergic neurons in the *Drosophila* brain. *Journal of Comparative Neurology, 513*(6), 643-667. doi:doi:10.1002/cne.21966

Cardona, A., Saalfeld, S., Preibisch, S., Schmid, B., Cheng, A., Pulokas, J., Tomancak, P., & Hartenstein, V. (2010). An Integrated Micro- and Macroarchitectural Analysis of the *Drosophila* Brain by Computer-Assisted Serial Section Electron Microscopy. *PLoS Biology, 8*(10), e1000502. doi:https://doi.org/10.1371/journal.pbio.1000502

Choi, Gloria B., Stettler, Dan D., Kallman, Benjamin R., Bhaskar, Shakthi T., Fleischmann, A., & Axel, R. (2011). Driving Opposing Behaviors with Ensembles of Piriform Neurons. *Cell, 146*(6), 1004-1015. doi:https://doi.org/10.1016/j.cell.2011.07.041

Christensen, T. A., & Hildebrand, J. G. (1987). Male-specific, sex pheromone-selective projection neurons in the antennal lobes of the moth *Manduca sexta*. *Journal of Comparative Physiology A, 160*(5), 553-569. doi:10.1007/bf00611929

Christensen, T. A., & Hildebrand, J. G. (1997). Coincident Stimulation With Pheromone Components Improves Temporal Pattern Resolution in Central Olfactory Neurons. *Journal of Neurophysiology, 77*(2), 775-781. doi:10.1152/jn.1997.77.2.775

Christensen, T. A., Mustaparta, H., & Hildebrand, J. G. (1991). Chemical communication in heliothine moths. *Journal of Comparative Physiology A, 169*(3), 259-274. doi:10.1007/bf00206990

Christensen, T. A., Mustaparta, H., & Hildebrand, J. G. (1995). Chemical communication in heliothine moths. *Journal of Comparative Physiology A, 177*(5), 545-557. doi:10.1007/bf00207184

Coates, K. E., Majot, A. T., Zhang, X., Michael, C. T., Spitzer, S. L., Gaudry, Q., & Dacks, A. M. (2017). Identified Serotonergic Modulatory Neurons Have Heterogeneous Synaptic Connectivity within the Olfactory System of *Drosophila*. *The Journal of Neuroscience, 37*(31), 7318-7331. doi:10.1523/jneurosci.0192-17.2017

Connolly, J. B., Roberts, I. J. H., Armstrong, J. D., Kaiser, K., Forte, M., Tully, T., & O'Kane, C. J. (1996). Associative Learning Disrupted by Impaired Gs Signaling in *Drosophila* Mushroom Bodies. *Science, 274*(5295), 2104-2107. doi:10.1126/science.274.5295.2104

Dacks, A. M., Christensen, T. A., & Hildebrand, J. G. (2006). Phylogeny of a serotonin-immunoreactive neuron in the primary olfactory center of the insect brain. *Journal of Comparative Neurology, 498*(6), 727-746. doi:10.1002/cne.21076

de Belle, J., & Heisenberg, M. (1994). Associative odor learning in Drosophila abolished by chemical ablation of mushroom bodies. *Science, 263*(5147), 692-695. doi:10.1126/science.8303280

Doty, R. L. (1986). Odor-guided behavior in mammals. *Experientia, 42*(3), 257-271.

Galizia, C. G., & Rössler, W. (2010). Parallel olfactory systems in insects: anatomy and function. *Annual Review of Entomology, 55*, 399-420. doi:10.1146/annurev-ento-112408-085442

Gatellier, L., Nagao, T., & Kanzaki, R. (2004). Serotonin modifies the sensitivity of the male silkmoth to pheromone. *Journal of Experimental Biology, 207*(14), 2487-2496. doi:10.1242/jeb.01035

Hammer, M. (1993). An identified neuron mediates the unconditioned stimulus in associative olfactory learning in honeybees. *Nature, 366*, 59. doi:10.1038/366059a0

Hammer, M., & Menzel, R. (1998). Multiple Sites of Associative Odor Learning as Revealed by Local Brain Microinjections of Octopamine in Honeybees. *Learning & Memory, 5*(1), 146-156.

Han, Q., Hansson, B. S., & Anton, S. (2005). Interactions of mechanical stimuli and sex pheromone information in antennal lobe neurons of a male moth, *Spodoptera littoralis*. *Journal of Comparative Physiology A, 191*(6), 521-528. doi:10.1007/s00359-005-0618-8

Hansson, B. S. (1995). Olfaction in Lepidoptera. *Experientia, 51*(11), 1003-1027. doi:10.1007/bf01946910

Hansson, B. S., Anton, S., & Christensen, T. A. (1994). Structure and function of antennal lobe neurons in the male turnip moth, *Agrotis segetum* (Lepidoptera: Noctuidae). *Journal of Comparative Physiology A, 175*(5), 547-562. doi:10.1007/bf00199476

Hansson, B. S., & Christensen, T. A. (1999). Functional Characteristics of the Antennal Lobe. In B. S. Hansson (Ed.), *Insect Olfaction* (1 ed., pp. 125-161). Germany: Springer.

Hansson, B. S., & Stensmyr, Marcus C. (2011). Evolution of Insect Olfaction. *Neuron, 72*(5), 698-711. doi:https://doi.org/10.1016/j.neuron.2011.11.003

Hartlieb, E., & Anderson, P. (1999). Olfactory-Released Behaviours. In B. S. Hansson (Ed.), *Insect Olfaction* (1 ed., pp. 315-349). Germany: Springer.

Hartlieb, E., Anton, S., & Hansson, B. S. (1997). Dose-dependent response characteristics of antennal lobe neurons in the male moth *Agrotis segetum* (Lepidoptera: Noctuidae). *Journal of Comparative Physiology A, 181*(5), 469-476. doi:10.1007/s003590050130

Heimbeck, G., Bugnon, V., Gendre, N., Keller, A., & Stocker, R. F. (2001). A central neural circuit for experience-independent olfactory and courtship behavior in *Drosophila* melanogaster. *Proceedings of the National Academy of Sciences, 98*(26), 15336-15341. doi:10.1073/pnas.011314898

Heinbockel, T., Christensen, T. A., & Hildebrand, J. G. (1999). Temporal tuning of odor responses in pheromone-responsive projection neurons in the brain of the sphinx moth *Manduca sexta*. *Journal of Comparative Neurology, 409*(1), 1-12. doi:doi:10.1002/(SICI)1096-9861(19990621)409:1<1::AID-CNE1>3.0.CO;2-7

Hildebrand, J. G., & Shepherd, G. M. (1997). MECHANISMS OF OLFACTORY DISCRIMINATION:Converging Evidence for Common Principles Across Phyla. *Annual Review of Neuroscience, 20*(1), 595-631. doi:10.1146/annurev.neuro.20.1.595

Hill, E. S., Iwano, M., Gatellier, L., & Kanzaki, R. (2002). Morphology and Physiology of the Serotonin-immunoreactive Putative Antennal Lobe Feedback Neuron in the Male

Silkmoth *Bombyx mori*. *Chemical Senses, 27*(5), 475-483. doi:10.1093/chemse/27.5.475

Homberg, U., Christensen, T. A., & Hildebrand, J. G. (1989). Structure and Function of the Deutocerebrum in Insects. *Annual Review of Entomology, 34*(1), 477-501. doi:10.1146/annurev.en.34.010189.002401

Homberg, U., Montague, R. A., & Hildebrand, J. G. (1988). Anatomy of antenno-cerebral pathways in the brain of the sphinx moth *Manduca sexta*. *Cell and Tissue Research, 254*(2), 255-281. doi:10.1007/bf00225800

Homberg, U., & Müller, U. (1999). Neuroactive Substances in the Antennal Lobe. In B. S. Hansson (Ed.), *Insect Olfaction* (1 ed., pp. 181-206). Germany: Springer.

Hoskins, S. G., Homberg, U., Kingan, T. G., Christensen, T. A., & Hildebrand, J. G. (1986). Immunocytochemistry of GABA in the antennal lobes of the sphinx moth *Manduca sexta*. *Cell and Tissue Research, 244*(2), 243-252. doi:10.1007/bf00219199

Ian, E., Berg, A., Lillevoll, S. C., & Berg, B. G. (2016a). Antennal-lobe tracts in the noctuid moth, *Heliothis virescens*: new anatomical findings. *Cell and Tissue Research, 366*(1), 23-35. doi:10.1007/s00441-016-2448-0

Ian, E., Zhao, X. C., Lande, A., & Berg, B. G. (2016b). Individual Neurons Confined to Distinct Antennal-Lobe Tracts in the Heliothine Moth: Morphological Characteristics and Global Projection Patterns. *Frontiers in Neuroanatomy, 10*(101). doi:10.3389/fnana.2016.00101

Ito, K., Shinomiya, K., Ito, M., Armstrong, J. D., Boyan, G., Hartenstein, V., Harzsch, S., Heisenberg, M., Homberg, U., Jenett, A., Keshishian, H., Restifo, Linda L., Rössler, W., Simpson, Julie H., Strausfeld, Nicholas J., Strauss, R., & Vosshall, Leslie B. (2014). A Systematic Nomenclature for the Insect Brain. *Neuron, 81*(4), 755-765. doi:https://doi.org/10.1016/j.neuron.2013.12.017

Iwano, M., Hill, E. S., Mori, A., Mishima, T., Mishima, T., Ito, K., & Kanzaki, R. (2010). Neurons associated with the flip-flop activity in the lateral accessory lobe and ventral protocerebrum of the silkworm moth brain. *Journal of Comparative Neurology, 518*(3), 366-388. doi:doi:10.1002/cne.22224

Jarriault, D., Gadenne, C., Rospars, J.-P., & Anton, S. (2009). Quantitative analysis of sex-pheromone coding in the antennal lobe of the moth *Agrotis ipsilon*: a tool to study network plasticity. *Journal of Experimental Biology, 212*(8), 1191-1201. doi:10.1242/jeb.024166

Jefferis, G. S. X. E., Potter, C. J., Chan, A. M., Marin, E. C., Rohlfing, T., Maurer, C. R., Jr., & Luo, L. (2007). Comprehensive Maps of *Drosophila* Higher Olfactory Centers: Spatially Segregated Fruit and Pheromone Representation. *Cell, 128*(6), 1187-1203. doi:10.1016/j.cell.2007.01.040

Kaissling, K. E. (2014). Pheromone Reception in Insects. In C. Mucignat-Caretta (Ed.), *Neurobiology of Chemical Communication*. USA: Taylor & Francis.

Kanzaki, R., Arbas, E. A., & Hildebrand, J. G. (1991). Physiology and morphology of protocerebral olfactory neurons in the male moth *Manduca sexta*. *Journal of Comparative Physiology A, 168*(3), 281-298. doi:10.1007/bf00198348

Kanzaki, R., Arbas, E. A., Strausfeld, N. J., & Hildebrand, J. G. (1989). Physiology and morphology of projection neurons in the antennal lobe of the male moth *Manduca sexta*. *Journal of Comparative Physiology A, 165*(4), 427-453. doi:10.1007/bf00611233

Kanzaki, R., Soo, K., Seki, Y., & Wada, S. (2003). Projections to Higher Olfactory Centers from Subdivisions of the Antennal Lobe Macroglomerular Complex of the Male Silkmoth. *Chemical Senses, 28*(2), 113-130. doi:10.1093/chemse/28.2.113

Kapoor, V., Provost, A. C., Agarwal, P., & Murthy, V. N. (2016). Activation of raphe nuclei triggers rapid and distinct effects on parallel olfactory bulb output channels. *Nature Neuroscience, 19*, 271. doi:doi:10.1038/nn.4219

Kay, L. M., & Stopfer, M. (2006). Information processing in the olfactory systems of insects and vertebrates. *Seminars in Cell & Developmental Biology, 17*(4), 433-442. doi:https://doi.org/10.1016/j.semcdb.2006.04.012

Keil, T. A. (1999). Morphology and Development of the Peripheral Olfactory Organs. In B. S. Hansson (Ed.), *Insect Olfaction* (1 ed., pp. 5-47). Germany: Springer.

Kent, K. S., Hoskins, S. G., & Hildebrand, J. G. (1987). A novel serotonin-immunoreactive neuron in the antennal lobe of the sphinx moth *Manduca sexta* persists throughout postembryonic life. *Journal of Neurobiology, 18*(5), 451-465. doi:10.1002/neu.480180506

King, J. R., Christensen, T. A., & Hildebrand, J. G. (2000). Response Characteristics of an Identified, Sexually Dimorphic Olfactory Glomerulus. *The Journal of Neuroscience, 20*(6), 2391-2399. doi:10.1523/jneurosci.20-06-02391.2000

Kloppenburg, P., Ferns, D., & Mercer, A. R. (1999). Serotonin Enhances Central Olfactory Neuron Responses to Female Sex Pheromone in the Male Sphinx Moth *Manduca*

sexta. *The Journal of Neuroscience, 19*(19), 8172-8181. doi:10.1523/jneurosci.19-19-08172.1999

Kloppenburg, P., & Mercer, A. R. (2008). Serotonin Modulation of Moth Central Olfactory Neurons. *Annual Review of Entomology, 53*(1), 179-190. doi:10.1146/annurev.ento.53.103106.093408

Kuebler, L., Olsson, S., Weniger, R., & Hansson, B. S. (2011). Neuronal Processing of Complex Mixtures Establishes a Unique Odor Representation in the Moth Antennal Lobe. *Frontiers in Neural Circuits, 5*(7). doi:10.3389/fncir.2011.00007

Laurent, G., & Davidowitz, H. (1994). Encoding of Olfactory Information with Oscillating Neural Assemblies. *Science, 265*(5180), 1872-1875. doi:10.1126/science.265.5180.1872

Lei, H., Anton, S., & Hansson, B. S. (2001). Olfactory protocerebral pathways processing sex pheromone and plant odor information in the male moth *Agrotis segetum*. *Journal of Comparative Neurology, 432*(3), 356-370. doi:doi:10.1002/cne.1108

Lei, H., Chiu, H.-Y., & Hildebrand, J. G. (2013). Responses of protocerebral neurons in *Manduca sexta* to sex-pheromone mixtures. *Journal of Comparative Physiology A, 199*(11), 997-1014. doi:10.1007/s00359-013-0844-4

Lei, H., & Hansson, B. S. (1999). Central Processing of Pulsed Pheromone Signals by Antennal Lobe Neurons in the Male Moth *Agrotis segetum*. *Journal of Neurophysiology, 81*(3), 1113-1122. doi:10.1152/jn.1999.81.3.1113

Livingstone, M., & Hubel, D. (1988). Segregation of form, color, movement, and depth: anatomy, physiology, and perception. *Science, 240*(4853), 740-749. doi:10.1126/science.3283936

Lizbinski, K. M., & Dacks, A. M. (2018). Intrinsic and Extrinsic Neuromodulation of Olfactory Processing. *Frontiers in Cellular Neuroscience, 11*(424). doi:10.3389/fncel.2017.00424

Løfaldli, B., Kvello, P., Kirkerud, N., & Mustaparta, H. (2012). Activity in Neurons of a Putative Protocerebral Circuit Representing Information about a 10 Component Plant Odor Blend in *Heliothis virescens*. *Frontiers in Systems Neuroscience, 6*(64). doi:10.3389/fnsys.2012.00064

Martin, J. P., Beyerlein, A., Dacks, A. M., Reisenman, C. E., Riffell, J. A., Lei, H., & Hildebrand, J. G. (2011). The neurobiology of insect olfaction: Sensory processing in a comparative context. *Progress in Neurobiology, 95*(3), 427-447. doi:https://doi.org/10.1016/j.pneurobio.2011.09.007

McBride, S. M. J., Giuliani, G., Choi, C., Krause, P., Correale, D., Watson, K., Baker, G., & Siwicki, K. K. (1999). Mushroom Body Ablation Impairs Short-Term Memory and Long-Term Memory of Courtship Conditioning in *Drosophila melanogaster*. *Neuron, 24*(4), 967-977. doi:https://doi.org/10.1016/S0896-6273(00)81043-0

Min, S., Ai, M., Shin, S. A., & Suh, G. S. B. (2013). Dedicated olfactory neurons mediating attraction behavior to ammonia and amines in *Drosophila*. *Proceedings of the National Academy of Sciences, 110*(14), E1321-E1329. doi:10.1073/pnas.1215680110

Mizunami, M., Nishino, H., & Yokohari, F. (2016). Status of and Future Research on Thermosensory Processing. *Frontiers in Physiology, 7*(150). doi:10.3389/fphys.2016.00150

Namiki, S., Iwabuchi, S., Pansopha Kono, P., & Kanzaki, R. (2014). Information flow through neural circuits for pheromone orientation. *Nature Communications, 5*, 5919. doi:10.1038/ncomms6919

Namiki, S., & Kanzaki, R. (2016). Comparative Neuroanatomy of the Lateral Accessory Lobe in the Insect Brain. *Frontiers in Physiology, 7*(244). doi:10.3389/fphys.2016.00244

Nara, K., Saraiva, L. R., Ye, X., & Buck, L. B. (2011). A Large-Scale Analysis of Odor Coding in the Olfactory Epithelium. *The Journal of Neuroscience, 31*(25), 9179-9191. doi:10.1523/jneurosci.1282-11.2011

Nassi, J. J., & Callaway, E. M. (2009). Parallel processing strategies of the primate visual system. *Nature Reviews Neuroscience, 10*, 360. doi:10.1038/nrn2619

Nässel, D. R. (1999). Histamine in the brain of insects: a review. *Microscopy Research and Technique, 44*, 121-136.

Okada, R., Awasaki, T., & Ito, K. (2009). Gamma-aminobutyric acid (GABA)-mediated neural connections in the *Drosophila* antennal lobe. *Journal of Comparative Neurology, 514*(1), 74-91. doi:doi:10.1002/cne.21971

Parnas, M., Lin, Andrew C., Huetteroth, W., & Miesenböck, G. (2013). Odor Discrimination in Drosophila: From Neural Population Codes to Behavior. *Neuron, 79*(5), 932-944. doi:10.1016/j.neuron.2013.08.006

Reisenman, C. E., Christensen, T. A., Francke, W., & Hildebrand, J. G. (2004). Enantioselectivity of Projection Neurons Innervating Identified Olfactory Glomeruli. *The Journal of Neuroscience, 24*(11), 2602-2611. doi:10.1523/jneurosci.5192-03.2004

Reisenman, C. E., Christensen, T. A., & Hildebrand, J. G. (2005). Chemosensory Selectivity of Output Neurons Innervating an Identified, Sexually Isomorphic Olfactory

Glomerulus. *The Journal of Neuroscience, 25*(35), 8017-8026. doi:10.1523/jneurosci.1314-05.2005

Reisenman, C. E., Dacks, A. M., & Hildebrand, J. G. (2011). Local interneuron diversity in the primary olfactory center of the moth *Manduca sexta*. *Journal of Comparative Physiology A, 197*(6), 653-665. doi:10.1007/s00359-011-0625-x

Root, C. M., Denny, C. A., Hen, R., & Axel, R. (2014). The participation of cortical amygdala in innate, odour-driven behaviour. *Nature, 515*, 269. doi:10.1038/nature13897

Rø, H., Müller, D., & Mustaparta, H. (2007). Anatomical organization of antennal lobe projection neurons in the moth *Heliothis virescens*. *The Journal of Comparative Neurology, 500*(4), 658-675. doi:10.1002/cne.21194

Røstelien, T., Borg-Karlson, A. K., Fäldt, J., Jacobsson, U., & Mustaparta, H. (2000). The Plant Sesquiterpene Germacrene D Specifically Activates a Major Type of Antennal Receptor Neuron of the Tobacco Budworm Moth *Heliothis virescens*. *Chemical Senses, 25*(2), 141-148. doi:10.1093/chemse/25.2.141

Røstelien, T., Stranden, M., Borg-Karlson, A. K., & Mustaparta, H. (2005). Olfactory Receptor Neurons in Two Heliothine Moth Species Responding Selectively to Aliphatic Green Leaf Volatiles, Aromatic Compounds, Monoterpenes and Sesquiterpenes of Plant Origin. *Chemical Senses, 30*(5), 443-461. doi:10.1093/chemse/bji039

Salecker, I., & Distler, P. (1990). Serotonin-immunoreactive neurons in the antennal lobes of the American cockroach *Periplaneta americana*: light- and electron-microscopic observations. *Histochemistry, 94*(5), 463-473. doi:10.1007/bf00272608

Sayin, S., Boehm, A. C., Kobler, J. M., De Backer, J.-F., & Grunwald Kadow, I. C. (2018). Internal State Dependent Odor Processing and Perception—The Role of Neuromodulation in the Fly Olfactory System. *Frontiers in Cellular Neuroscience, 12*(11). doi:10.3389/fncel.2018.00011

Seki, Y., Aonuma, H., & Kanzaki, R. (2005). Pheromone processing center in the protocerebrum of *Bombyx mori* revealed by nitric oxide-induced anti-cGMP immunocytochemistry. *Journal of Comparative Neurology, 481*(4), 340-351. doi:doi:10.1002/cne.20392

Shorey, H. H. (1973). Behavioral Responses to Insect Pheromones. *Annual Review of Entomology, 18*(1), 349-380. doi:10.1146/annurev.en.18.010173.002025

Stengl, M. (2010). Pheromone Transduction in Moths. *Frontiers in Cellular Neuroscience, 4*(133). doi:10.3389/fncel.2010.00133

Stengl, M., Ziegelberger, G., Beoekhoff, I., & Krieger, J. (1999). Perireceptor Event and Transduction Mechanisms in Insect Olfaction. In B. S. Hansson (Ed.), *Insect Olfaction* (1 ed., pp. 49-96). Germany: Springer.

Stopfer, M. (2014). Central processing in the mushroom bodies. *Current Opinion in Insect Science, 6*, 99-103. doi:https://doi.org/10.1016/j.cois.2014.10.009

Stranden, M., Liblikas, I., König, W. A., Almaas, T. J., Borg-Karlson, A.-K., & Mustaparta, H. (2003a). (–)-Germacrene D receptor neurones in three species of heliothine moths: structure-activity relationships. *Journal of Comparative Physiology A, 189*(7), 563-577. doi:10.1007/s00359-003-0434-y

Stranden, M., Røstelien, T., Liblikas, I., Almaas, T. J., Borg-Karlson, A.-K., & Mustaparta, H. (2003b). Receptor neurones in three heliothine moths responding to floral and inducible plant volatiles. *Chemoecology, 13*(3), 143-154. doi:10.1007/s00049-003-0242-4

Strutz, A., Soelter, J., Baschwitz, A., Farhan, A., Grabe, V., Rybak, J., Knaden, M., Schmuker, M., Hansson, B. S., & Sachse, S. (2014). Decoding odor quality and intensity in the *Drosophila* brain. *eLife, 3*, e04147. doi:10.7554/eLife.04147

Sun, X., Tolbert, L. P., & Hildebrand, J. G. (1993). Ramification Pattern and Ultrastructural Characteristics of the Serotonin-Immunoreactive Neuron in the Antennal Lobe of the Moth *Manduca Sexta* : A Laser-Scanning Confocal and Electron-Microscopic Study. *Journal of Comparative Neurology, 338*(1), 5-16.

Tanaka, N. K., Endo, K., & Ito, K. (2012a). Organization of antennal lobe-associated neurons in adult *Drosophila* melanogaster brain. *Journal of Comparative Neurology, 520*(18), 4067-4130. doi:doi:10.1002/cne.23142

Tanaka, N. K., Suzuki, E., Dye, L., Ejima, A., & Stopfer, M. (2012b). Dye Fills Reveal Additional Olfactory Tracts in the Protocerebrum of Wild-Type *Drosophila*. *The Journal of Comparative Neurology, 520*(18), 4131-4140. doi:10.1002/cne.23149

Vickers, N. J. (2006). Winging It: Moth Flight Behavior and Responses of Olfactory Neurons Are Shaped by Pheromone Plume Dynamics. *Chemical Senses, 31*(2), 155-166. doi:10.1093/chemse/bjj011

Vickers, N. J., & Christensen, T. A. (2003). Functional Divergence of Spatially Conserved Olfactory Glomeruli in Two Related Moth Species. *Chemical Senses, 28*(4), 325-338. doi:10.1093/chemse/28.4.325

Vosshall, L. B. (2000). Olfaction in *Drosophila*. *Current Opinion in Neurobiology, 10*(4), 498-503. doi:https://doi.org/10.1016/S0959-4388(00)00111-2

Vosshall, L. B., Wong, A. M., & Axel, R. (2000). An Olfactory Sensory Map in the Fly Brain. *Cell, 102*(2), 147-159. doi:https://doi.org/10.1016/S0092-8674(00)00021-0

Wang, K., Gong, J., Wang, Q., Li, H., Cheng, Q., Liu, Y., Zeng, S., & Wang, Z. (2014). Parallel pathways convey olfactory information with opposite polarities in *Drosophila*. *Proceedings of the National Academy of Sciences, 111*(8), 3164-3169. doi:10.1073/pnas.1317911111

Wernecke, K. E. A., Vincenz, D., Storsberg, S., D'Hanis, W., Goldschmidt, J., & Fendt, M. (2015). Fox urine exposure induces avoidance behavior in rats and activates the amygdalar olfactory cortex. *Behavioural Brain Research, 279*, 76-81. doi:https://doi.org/10.1016/j.bbr.2014.11.020

Wilson, R. I., & Mainen, Z. F. (2006). Early Events in Olfactory Processing. *Annual Review of Neuroscience, 29*(1), 163-201. doi:10.1146/annurev.neuro.29.051605.112950

Wu, W., Anton, S., Löfstedt, C., & Hansson, B. S. (1996). Discrimination among pheromone component blends by interneurons in male antennal lobes of two populations of the turnip moth, *Agrotis segetum*. *Proceedings of the National Academy of Sciences, 93*(15), 8022-8027. doi:10.1073/pnas.93.15.8022

Wyatt, T. D. (2003). Sex pheromones: finding and choosing mates. In *Pheromones and Animal Behaviour* (1 ed., pp. 37-73). USA: Cambridge University Press.

Yaksi, E., & Wilson, R. I. (2010). Electrical Coupling between Olfactory Glomeruli. *Neuron, 67*(6), 1034-1047. doi:https://doi.org/10.1016/j.neuron.2010.08.041

Zhang, X., & Gaudry, Q. (2016). Functional integration of a serotonergic neuron in the *Drosophila* antennal lobe. *eLife, 5*, e16836. doi:10.7554/eLife.16836

Zhao, X. C., & Berg, B. G. (2009). Morphological and physiological characteristics of the serotonin-immunoreactive neuron in the antennal lobe of the male oriental tobacco budworm, *Helicoverpa assulta*. *Chemical Senses, 34*(5), 363-372. doi:10.1093/chemse/bjp013

Zhao, X. C., & Berg, B. G. (2010). Arrangement of Output Information from the 3 Macroglomerular Units in the Heliothine Moth *Helicoverpa assulta*: Morphological and Physiological Features of Male-Specific Projection Neurons. *Chemical Senses, 35*(6), 511-521. doi:10.1093/chemse/bjq043

Zhao, X. C., Kvello, P., Løfaldli, B. B., Lillevoll, S. C., Mustaparta, H., & Berg, B. G. (2014). Representation of pheromones, interspecific signals, and plant odors in higher olfactory centers; mapping physiologically identified antennal-lobe projection neurons

in the male heliothine moth. *Frontiers in Systems Neuroscience, 8*(186). doi:10.3389/fnsys.2014.00186

Zhao, X. C., Ma, B.-W., Berg, B. G., Xie, G.-Y., Tang, Q.-B., & Guo, X.-R. (2016). A global-wide search for sexual dimorphism of glomeruli in the antennal lobe of female and male Helicoverpa armigera. *Scientific Reports, 6*, 35204. doi:10.1038/srep35204

Zhao, X. C., Pfuhl, G., Surlykke, A., Tro, J., & Berg, B. G. (2013a). A multisensory centrifugal neuron in the olfactory pathway of heliothine moths. *Journal of Comparative Neurology, 521*(1), 152-168. doi:10.1002/cne.23166

Zhao, X. C., Tang, Q.-B., Berg, B. G., Liu, Y., Wang, Y.-R., Yan, F.-M., & Wang, G.-R. (2013b). Fine structure and primary sensory projections of sensilla located in the labial-palp pit organ of *Helicoverpa armigera* (Insecta). *Cell and Tissue Research, 353*(3), 399-408. doi:10.1007/s00441-013-1657-z

Appendix A

Projection neurons in the medial antennal lobe tract

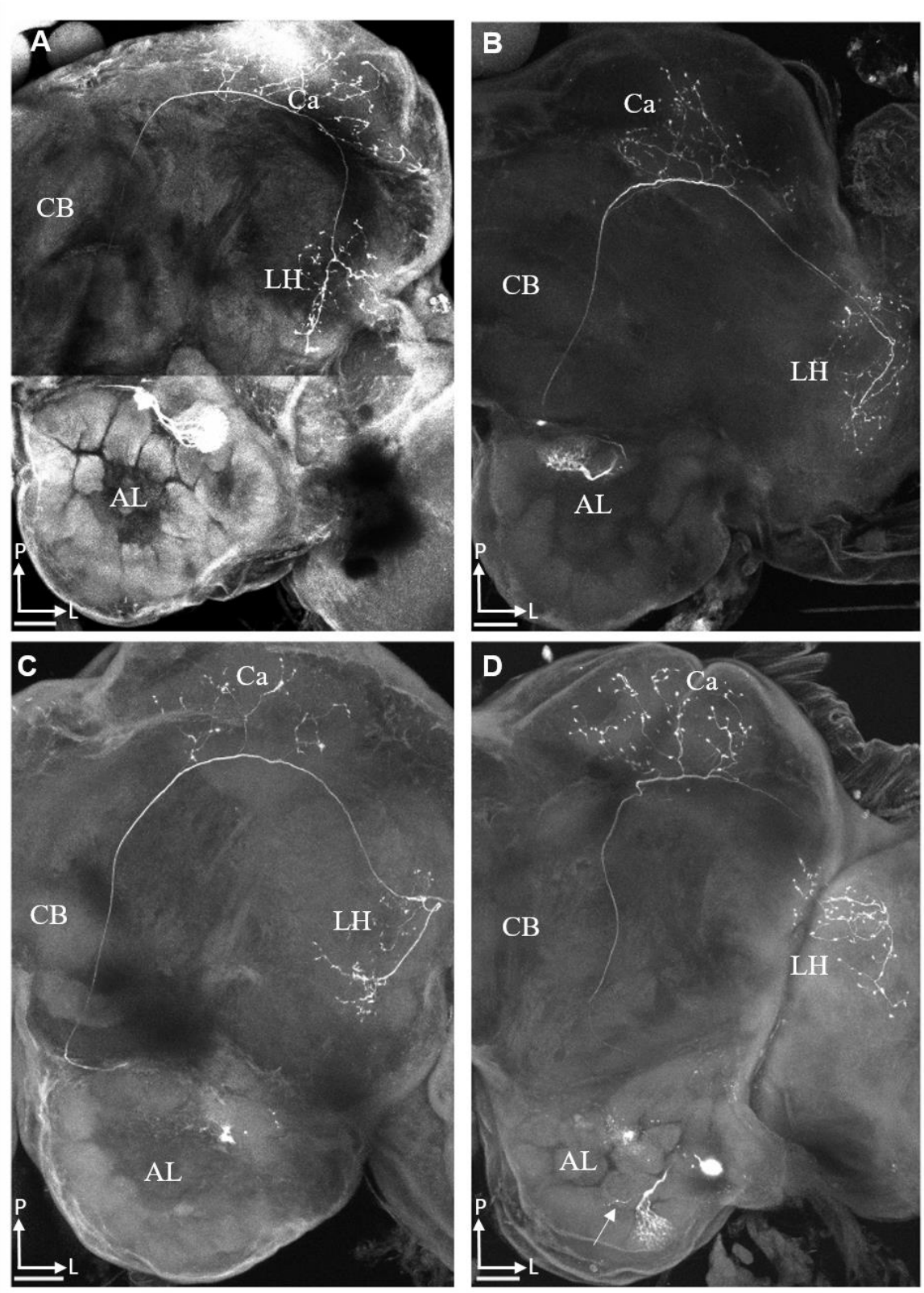

Appendix Figure 1. Confocal images of four uniglomerular projection neurons (PNs) in the medio-lateral antennal lobe tract (m-ALT), in dorsal view. **(A-B)** Each individual PN (#5, 4) had the soma

located in the medial cell cluster and innervated an ordinary glomerulus (OG). Their terminal output connections in the protocerebrum where confined to the calyces (Ca) and the lateral horn (LH). **(C)** OG PN (#10) in the m-ALT which projected to the calyces and the LH. Soma was not stained. **(D)** PN (#1) with the soma in the lateral cell cluster. In addition to innervating an OG, this PN also extended a neurite into an adjacent glomerulus (arrow). Terminal projections in the protocerebrum were observed in the calyces and the LH. CB, central body. Scale bars: 50 µm.

Appendix B

Projection neurons in the medial, medio-lateral, and lateral antennal lobe tract

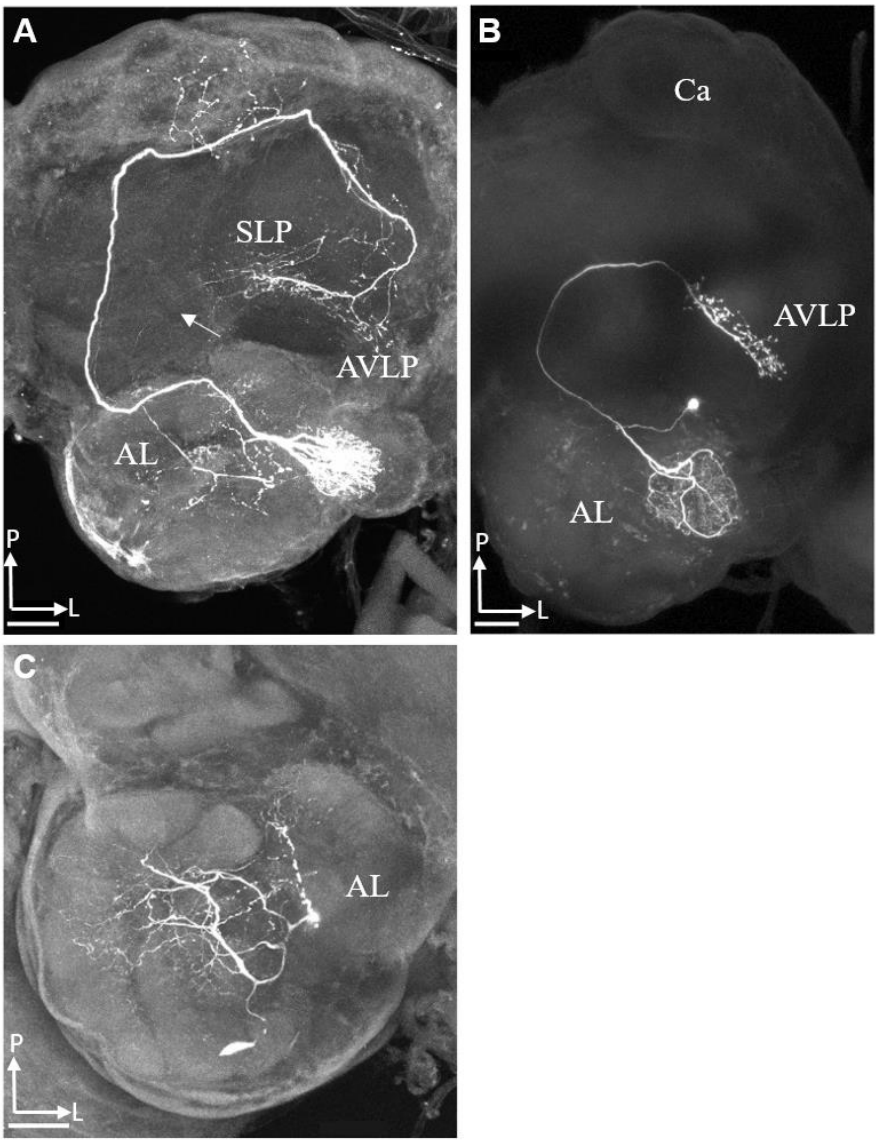

Appendix Figure 2. Confocal images of projection neurons (PNs) in the medial antennal lobe tract (m-ALT) (A), medio-lateral antennal lobe tract (ml-ALT) (B), and lateral antennal lobe tract (l-ALT) (C), in dorsal view. **(A)** A PN innervated the cumulus unit of the macroglomerular complex, projected in the m-ALT and terminated in the anterior ventro-lateral protocerebrum (AVLP) and superior lateral protocerebrum (SLP) (soma not stained). Additionally, one l-ALT PN can be seen (arrow). **(B)** A multiglomerular PN (#20) in the ml-ALT had soma in the lateral cell cluster and innervated the MGC. Terminal projections were observed in the AVLP. **(C)** A single PN innervated multiple ordinary glomeruli (OG) in the antennal lobe (AL) and had soma located in the anterior cell cluster. Primary neurite is not shown due to weak staining. Ca, calyces. Scale bars: 50 µm.

Appendix C

Projection neurons which were inhibited by the sunflower extract all innervate glomeruli in the same region of the antennal lobe

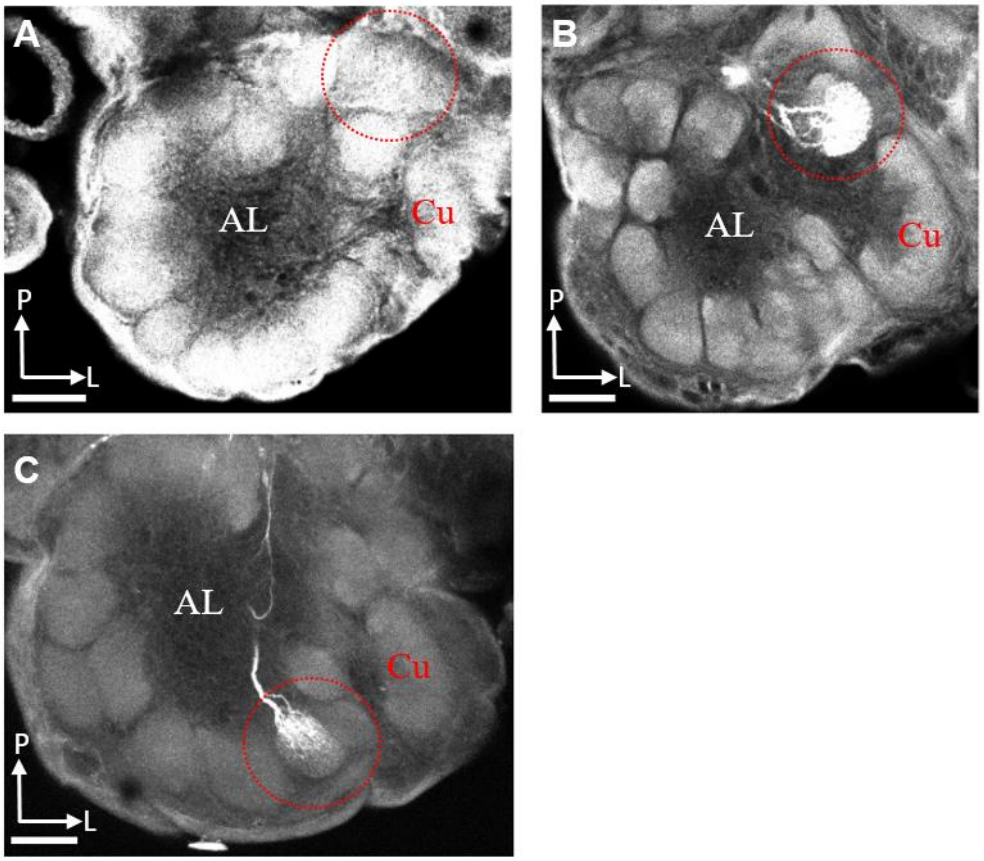

Appendix Figure 3. Projection neurons (PNs) responding to sunflower extract all innervated glomeruli is a specific region of the antennal lobe (AL). **(A-C)** Three PNs which all exhibited inhibition to the sunflower extract all had dendrites in glomeruli located in the same dorso-lateral region of the AL, close to the cumulus (Cu) unit of the macroglomerular complex. Scale bar: 50 µm.

Appendix D

Raw data showing the physiological responses of the bilateral, paired centrifugal neurons to odorant stimuli and control

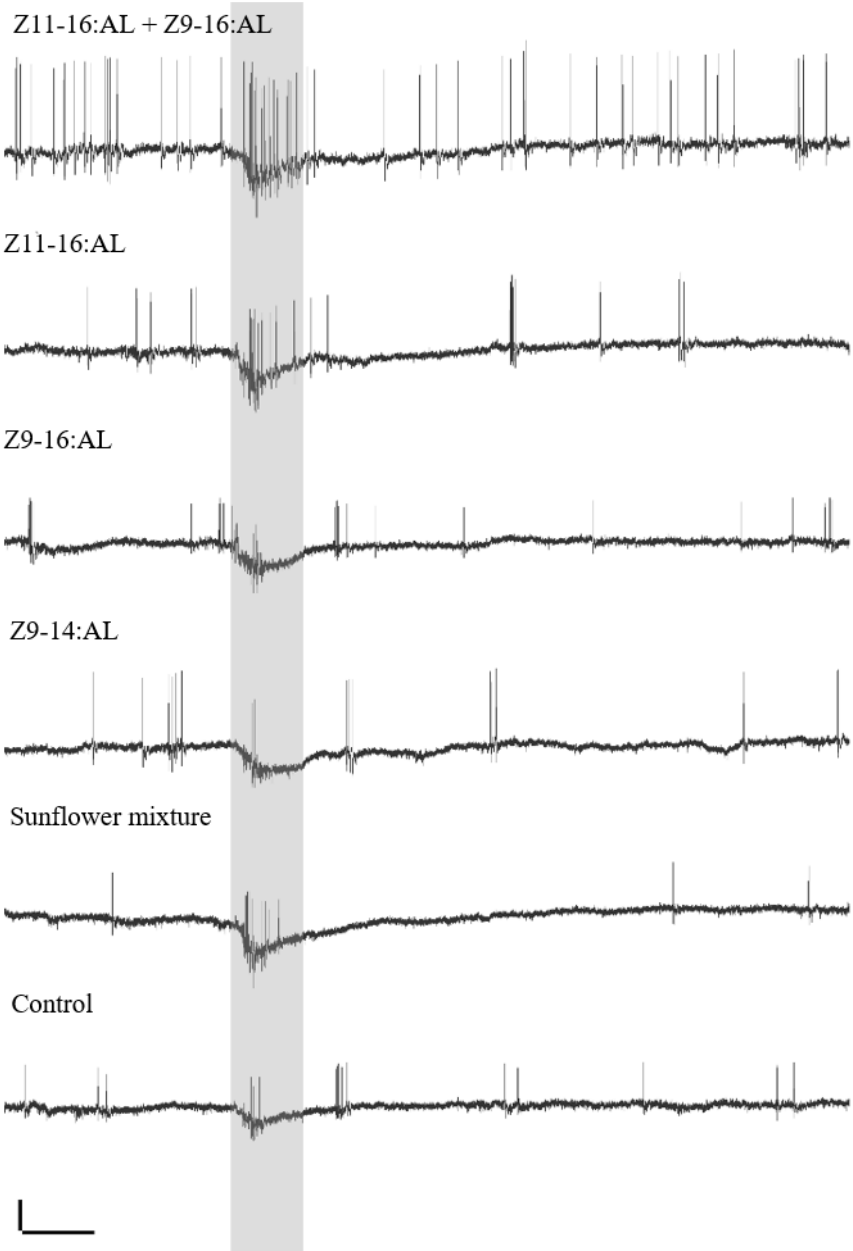

Appendix Figure 4. Raw data from the bilateral, paired centrifugal neuron. Note the increase in spikes to the 95:5 blend of the primary (Z11-16:AL) and secondary (Z9-16:AL) pheromone component, the primary (Z11-16:AL) pheromone component and sunflower extracts. Remaining stimuli elicits no increase in firing frequencies. Scale bar: 10mV, 400ms.